

## Accounts

---

### Nanoscale Molecular Containers

Dmitry M. Rudkevich

The Department of Chemistry and Biochemistry, The University of Texas at Arlington,  
Box 19065, Arlington, TX 76019, USA

(Received April 2, 2001)

Over the last few years, there has been a breakthrough in the design and synthesis of nanoscale molecular containers—cavitands, (hemi)carcerands, and capsules. These nanocavities are designed for selective binding, separation and sensing of smaller molecules and ions, molecular transport and delivery, stabilization of reactive intermediates, and catalysis through encapsulation. They also mimic the hydrophobic pockets of enzymes. The field has grown since the first hollow calixarenes of Collet, Cram, and Gutsche, which were able to trap a single solvent or gas molecule, in the early 1980s, to investigations of giant cavities of 15–20 Å inner dimensions and 1500 Å<sup>3</sup> internal volume. This reflects current trends in molecular recognition which are rapidly moving towards nanotechnology and microfabrication on the one hand and molecular biology on the other. Recently prepared nanocavities are ready to be employed for encapsulation of drugs and their active transport/delivery through cell membranes. Cavity-containing informationally rich polymers, sensing materials and polymer-supported microreactors are also in sight. These and many other applications can only be possible if general approaches towards construction of nanoscale molecular containers are developed and if the key rules governing their inclusion complexes are understood at the level of their organic chemistry.

In biological substrate-receptor complexes, binding sites of enzymes or nucleic acids possess convergent, concave surfaces, and synthetic cavities are their counterparts in molecular recognition.<sup>1</sup> Their significance for studying complexation processes is also somewhat comparable to the significance of macroscopic cavities in our daily life. The interest of organic chemists in three-dimensional, cavity-containing hosts dates to the work of Cramer on the inclusion complexes of cyclodextrins in 1950s.<sup>2</sup> However the contemporary progress in this area has been, without any doubt, stimulated by the research of Cram and his co-workers on molecular containers.<sup>3</sup>

In contrast to cyclodextrins,<sup>4</sup> cyclophanes,<sup>5</sup> macrocyclic cages,<sup>6</sup> and cleft-type receptors<sup>7</sup> which are relatively flexible and possess significant openings in their structures, Cram's containers offered rigid and shielded from the bulk solution polyaromatic, inner cavities able to entrap smaller species. *Cavitands* are synthetic host-molecules with open-ended enforced cavities large enough to bind complementary organic molecules and ions.<sup>8</sup> The concave inner surfaces of cavitands can be designed to have various shapes, with either integrated or appended binding sites. Complexes of cavitands are called *caviplexes*. *Carcerands* are close-surface host-molecules with enforced inner cavities which are large enough to incarcerate smaller organic molecules, and portals of which are too narrow to allow the guest to escape without breaking covalent bonds.<sup>9</sup> Complexes of carcerands, *carceplexes*, represent an extreme form of host-guest complex stabilities. Carcerands hold guests

permanently. In fact, most carceplexes include guests during their synthesis—upon covalent shell-closure; guests can often template the synthetic process. *Hemicarceplexes* are carceplexes with larger portals, which allow for the entrapped guest to escape at high temperature, but to remain incarcerated under conditions of their isolation and characterization at ordinary temperatures.<sup>10</sup> Guest-free hemicarceplexes are called *hemicarcerands*. The differences among cavitands, carcerands and hemicarcerands are in their ease of guest uptake and release—the exchange rates. More recently, *self-assembling capsules* emerged; these are receptors with enclosed cavities formed through the reversible noncovalent interactions between two or more subunits.<sup>11,12</sup> Likewise (hemi)carcerands, capsules completely surround their guests but may release them without breaking covalent bonds and under much milder conditions. Over the last fifteen years, the desirability of controlling the cavity's size and shape has led to the successful synthesis of various molecular containers and their complexes.<sup>13–16</sup> Eventually it became obvious that aiming at drug delivery, stabilization of reactive intermediates, and catalysis would require much larger cavities. Even simple, biologically important molecules—carbohydrates, nucleotides, steroids, oligopeptides—and drugs are relatively large: of > 10 Å (> 1 nm) in length and > 300 Daltons in molecular weight. Catalytic reactions most often require at least two molecules placed in a close proximity. Unlike some alternative cavity-forming structures employed in chemistry, biochemistry and molecular biol-

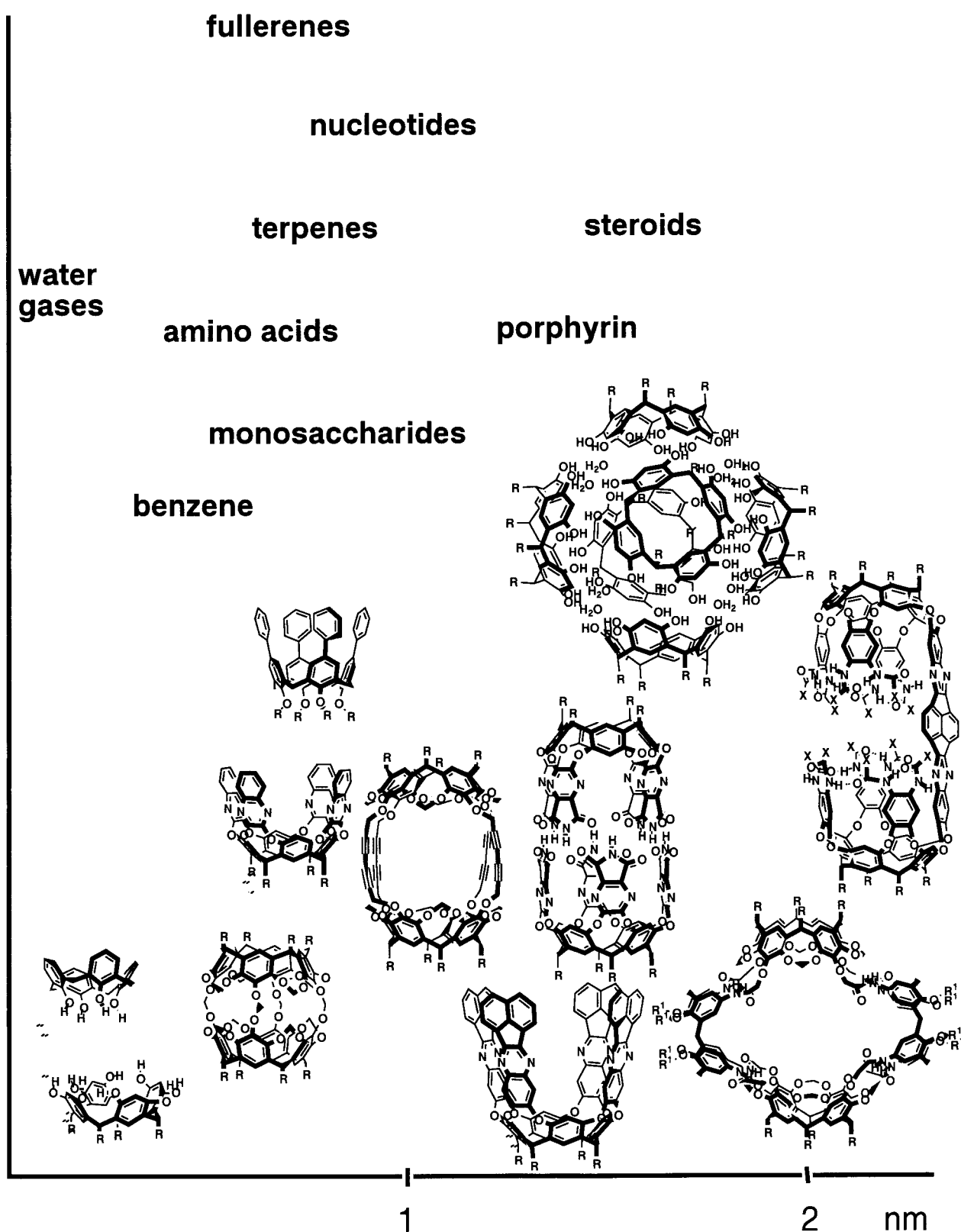


Fig. 1. Inner cavity dimensions of known molecular containers compared with dimensions of different classes of organic substances.

ogy—imprinted polymers and dendrimers,<sup>17</sup> liposomes,<sup>18</sup> zeolites,<sup>19</sup> and catalytic antibodies<sup>20</sup>—most of the early cavitands, (hemi)carcerands, and self-assembling capsules had moderate

interior dimensions (Fig. 1). They could only embrace a single, solvent-size organic molecule. Moreover, their cavities were poorly functionalized.

The quest for engineering (supra)molecular cavities of *nanoscale* dimensions had thus emerged. In this review, we summarize the most recent efforts and exciting developments that have led to the next generation of synthetic molecular containers—nanoscale cavities, those with inner space large enough to entrap guests of nanoscale ( $\geq 10$  Å, or  $\geq 1$  nm) dimensions or several regular-sized organic molecules. The analysis will be developed on the basis of the increasing complexity of the host's structures, which is determined by the capability to form stable and/or selective molecule-within-molecule aggregates. Usually, molecular recognition complexes depend on stereoelectronic complementarity between receptor and substrate and are held together by hydrogen bonding, metal–ligand attractions, ion–ion, ion–dipole, CH– $\pi$  and  $\pi$ – $\pi$  interactions, van der Waals and solvophobic forces.<sup>21</sup> In contrast, carceplexes, hemicarceplexes, self-assembling capsules, and, to a less extent, caviplexes rely first of all on so-called *constrictive binding*:<sup>22</sup> the stability of these complexes is mostly provided not through the intrinsic host–guest attraction but through mechanical inhibition of the decomplexation process. According to Cram,<sup>22</sup> constrictive binding is:

$$\Delta G^{\#}_{\text{constrictive}} = \Delta G^{\#}_{\text{assoc}} = \Delta G^{\#}_{\text{dissoc}} - (-\Delta G^{\circ}),$$

where  $\Delta G^{\#}_{\text{assoc}}$  and  $\Delta G^{\#}_{\text{dissoc}}$  are the free energies of activation for the complex formation and dissociation, respectively, and  $-\Delta G^{\circ}$  is the intrinsic host–guest binding energy. For a medium-sized hemicarceplex, it was experimentally demonstrated that most of the constrictive binding comes from the host's structural reorganization.<sup>22</sup> Both the inner cavity dimensions and its opening/portal's size and rigidity have a significant influence on  $\Delta G^{\#}_{\text{assoc}}$  and  $\Delta G^{\#}_{\text{dissoc}}$  activation energies. Enlarging the cavity often leads to the host's higher flexibility. The kinetic stability of the complexes decreases when the portals are widely open, allowing the guest to escape easily. At the same time, very rigid and preorganized portals may prevent the guest entering.

Both the guest's size and its shape reflect the binding ability of the hosts. In the absence of additional intermolecular forces, recognition-through-encapsulation is largely determined by the host and guest volumes. Competition with the solvent molecules situated inside the cavity may be one important reason to block the guests entering. Accordingly, the  $\Delta G^{\#}_{\text{assoc}}$  barriers can be decreased by using a solvent with minimal solvating ability. In addition, "very large" solvent molecules, which are not able to fit inside the cavity or are simply too bulky to pass through the portals, can be used. And finally, the introduction of additional binding sites within the interior increases the  $-\Delta G^{\circ}$  intrinsic binding free energy. Up to date, this remains a challenging synthetic task.

Following the established traditions in this field, we will overview all main classes of cavities—open-ended, partially sealed, and completely sealed nanoscale molecular containers. The use of both covalent forces and noncovalent interactions in the cavity-forming processes will be discussed. We will also thoroughly address the special consequences that the cavity dimensions hold for the guest inclusion.<sup>23</sup> Molecular recognition is developing so rapidly that almost every day brings a new receptor or a host–guest complex; both organic

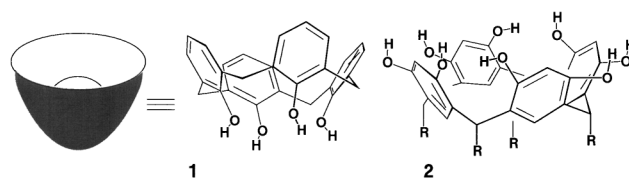


Fig. 2. Calix[4]arene **1** and resorcinarene **2** as bowl-shaped modules for construction of deep cavitands.

and inorganic building blocks are involved in the construction. We will therefore limit our discussion to examples from the calixarene chemistry (see **1** and **2**, Fig. 2). Technically, calixarenes readily provide features for the construction of nanocavities. Their three-dimensional and rigid structure, concave and potentially extendable polyaromatic surfaces, commercial availability, and extremely rich preparative chemistry make them traditional, convenient platforms for synthetic elaboration.<sup>24</sup> There is also a historical reason: a vast majority of the early molecular containers were based on calixarenes and their relatives—resorcinarenes and cyclotrimeratrylenes.<sup>3,25</sup> At the same time we believe that similar principles and rules are, in general, applicable for designing and studying of a wide variety of other nano-sized cavities, boxes, channels, etc.

## 1. Construction of Deep Cavitands

Calixarenes and resorcinarenes are conformationally flexible and do not have enforced cavities.<sup>25</sup> In the early generations of cavitands, the crown  $C_{4v}$  conformation of resorcinarene **2** was rigidly fixed by four alkylendioxy- and dialkylsilylcon bridges;<sup>26</sup> this generated well-defined, vase-shaped cavities **3** (Fig. 3). Likewise, the calix[4]arene **1** aromatic rings were fixed in the perfect cone conformation through the covalent bridging of proximal phenol oxygens with diethylene glycolic chains.<sup>27</sup> This resulted in calix[4]arene bis(crown-3) **4** (Fig. 3). Compared to their flexible precursors, cavitands **3** and **4** showed better affinity towards small organic molecules/solvents, alkylammonium cations and *N*-methylpyridinium in solution and in the solid state. For example, in the X-ray structure of the complex of *p*-cyclohexylcalix[4]arene bis(crown-3) **5** with  $\text{CH}_3\text{NO}_2$  the guest is situated within the cavity, with its

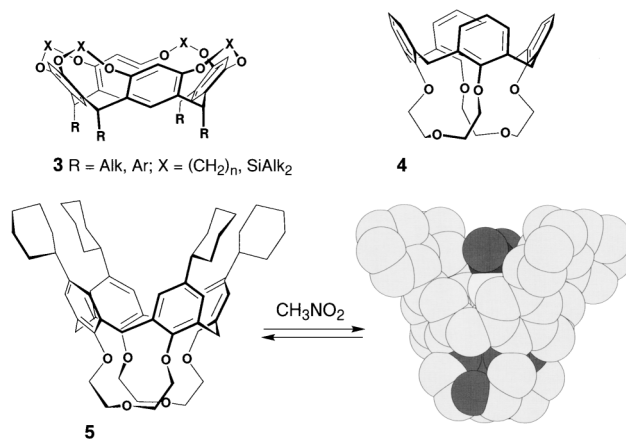


Fig. 3. Top: covalently rigidified cavitands **3**<sup>26</sup> and **4**.<sup>27</sup> Bottom: X-ray structure of complex **5**· $\text{CH}_3\text{NO}_2$ .<sup>27</sup>

CH<sub>3</sub> group buried inside the aromatic skeleton (Fig. 3).<sup>27</sup> In CDCl<sub>3</sub> and CCl<sub>4</sub> solution, cavitand **5** binds CH<sub>3</sub>NO<sub>2</sub> better than its flexible analogs.

Much more important, however, is the use of cavitands **3** and **4** in the construction of larger and deeper molecular containers. Indeed, in most of the crystal structures of the inclusion complexes of calixarenes and derived from them smaller cavitands, the guest molecule is positioned not inside but roughly above the plane defined by the upper carbon atoms of the cyclic polyaromatic skeleton.<sup>3,24,26</sup> The cavity's depth is generally less than 4 Å, which leaves room only for one methyl-sized fragment to be included. Accordingly, several approaches have been developed to enlarge the cavity and achieve better guest entrapment (Fig. 4). Direct *C*-arylation of the aromatic rings in calixarenes and resorcinarenes provides one attractive route towards larger ( $\geq 10$  Å) hydrophobic platforms and cavities (see for example, **6** and **7**, Figs. 4 and 5). So-called "deep cavity" calixarenes were initially prepared by Gutsche in 1985 via step-wise condensation of biphenyl-4-ol and formaldehyde, but the yields were low ( $< 14\%$ ).<sup>28</sup> More recently, the aryl walls were attached to already preformed calixarenes via thallium-, mercury-, zinc/nickel(0)-, and boron-mediated syntheses.<sup>29</sup> Subsequently, conformationally rigid bis(crown-3) derivatives of calix[4]arenes were made available.<sup>27</sup> Likewise, the cavities in resorcinarene-based cavitands were deepened through *C*-arylation in the 2'-position of the resorcinarene rings, using the Suzuki and Stille reactions.<sup>30–32</sup> The *p*- and *m*-substituents at the upper rims of deep platforms and cavitands **6** and **7** were successfully used for further derivatization. For example, triethylene glycol footed deep cavitands **8** (Fig. 6) is functionalized with four *m*-amidinium groups at the upper rim and effectively binds nucleotides

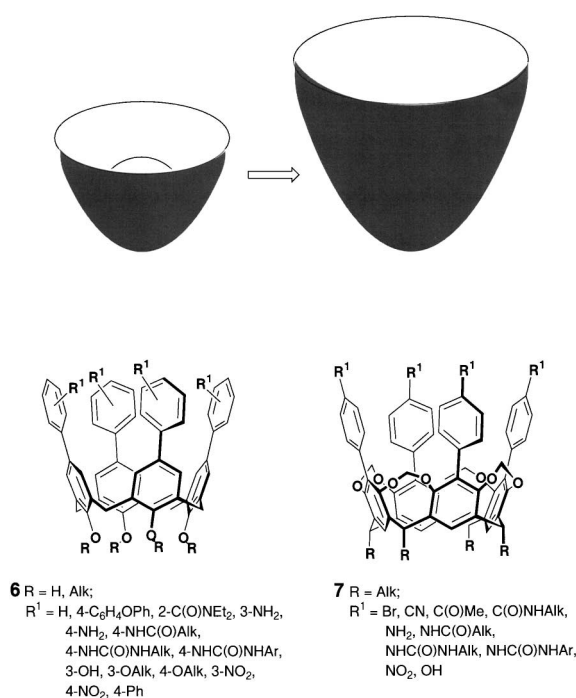


Fig. 4. Deepening cavitands—a cartoon. Bottom: deep calix[4]arenes **6**<sup>29,31</sup> and deep cavitands **7**.<sup>30,31</sup>

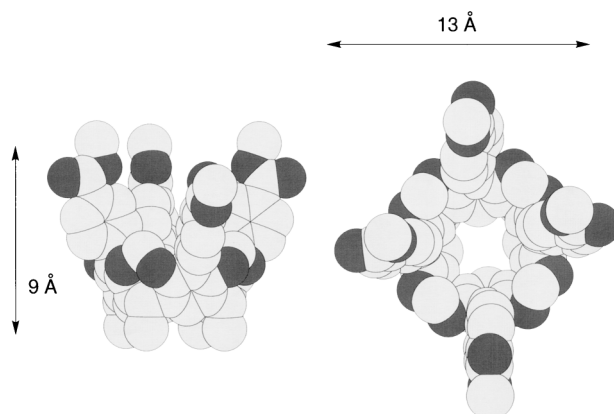


Fig. 5. X-ray structure of deep cavitand **7** (R<sup>1</sup> = C(O)Me).<sup>30</sup> Here and further in the legends, the CH hydrogen atoms and long alkyl chains are omitted for viewing clarity.

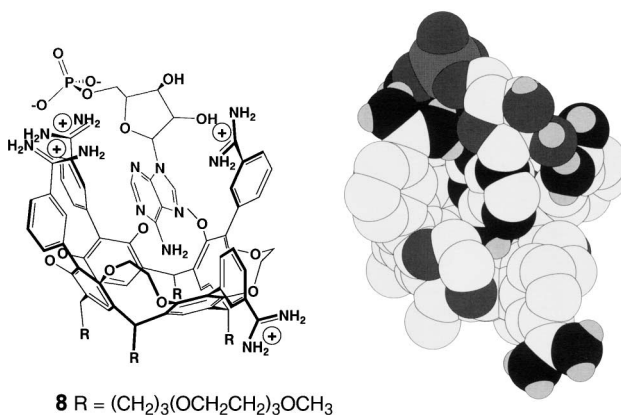
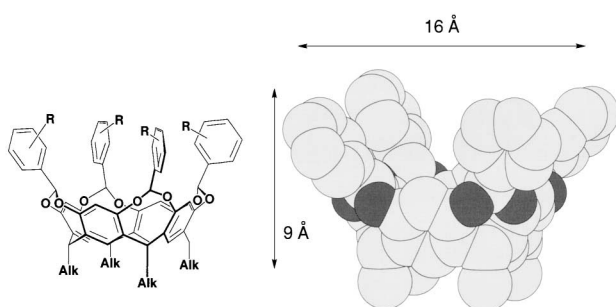


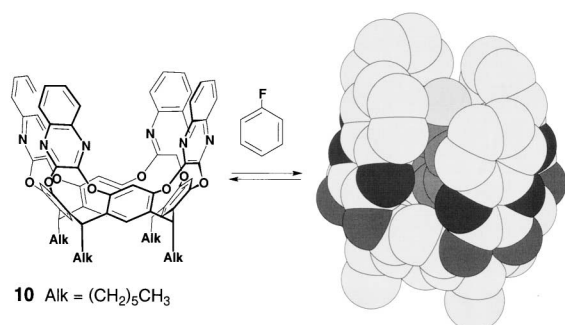
Fig. 6. Proposed complex of cavitand **8** with AMP.<sup>32</sup> Right: energy-minimized structure of the complex in H<sub>2</sub>O.<sup>32</sup> For simplicity, the (CH<sub>2</sub>)<sub>3</sub>(OCH<sub>2</sub>CH<sub>2</sub>)<sub>3</sub>OCH<sub>3</sub> lower chains are replaced by CH<sub>3</sub> groups.

and even dinucleotides in buffered aqueous and methanol solutions.<sup>37</sup> For adenine nucleotides, the association constant ( $K_{\text{ass}}$ ) values in a range  $1.4 \times 10^3 - 6.6 \times 10^5 \text{ M}^{-1}$  were determined by <sup>1</sup>H NMR spectroscopy (<sup>2</sup>H<sub>2</sub>O, pH 8.3, 300 K). In addition to charged interactions and hydrogen bonding, the cavity also contributes to the overall binding process. The analysis of NMR chemical shifts as well as molecular modeling strongly suggest that the adenine fragment is situated deep inside host **8**.<sup>32</sup>

Another strategy to deepen cavitands includes modification of the linkers between the resorcinarene's aromatic walls (Fig. 7). The most recent accomplishment in this direction is a family of deep cavitands **9**.<sup>33</sup> These were prepared in the reaction between resorcinarene **2** (R = CH<sub>2</sub>CH<sub>2</sub>Ph) and various benzylidene dibromides and subsequently used for the construction of nanoscale hemicarcerands. Condensation of resorcinarenes with 2,3-dichloroquinoxaline built cavitand **10** with more extended walls and a shielded inner cavity (Fig. 7).<sup>34,35</sup> According to the X-ray analysis, molecule **10** possesses a lipophilic cavity 7.2 Å wide and 8.3 Å deep, which is large enough to accommodate aromatic molecules.<sup>34</sup> Such guests as CH<sub>2</sub>Cl<sub>2</sub> and fluorobenzene were seen inside cavitand **10** in the solid



**9** Alk = (CH<sub>2</sub>)<sub>2</sub>Ph; R = H, 2-Br, 3-Br, 3-Me, 3-OCH<sub>2</sub>OEt, 3-NO<sub>2</sub>, 3-CN, 4-Br, 4-I, 4-Me, 4-OH, 4-Ph, 4-CN, etc.



**10** Alk = (CH<sub>2</sub>)<sub>5</sub>CH<sub>3</sub>

Fig. 7. Top: extended cavitand **9** and its X-ray structure.<sup>33</sup> Bottom: cavitand **10** and X-ray structure of complex **10**·Fluorobenzene.<sup>34</sup>

state by X-ray crystallography.<sup>34,35</sup> The complexation-decomplexation process in solution was fast on the NMR time-scale, and only time-averaged chemical shifts were seen when binding occurred. For aromatic guests, the binding energies of  $-\Delta G^{298} = 2.0\text{--}3.1$  kcal/mol (1 cal  $\approx$  4.18 J) were measured for a 1:1 complex with **10** in [D<sub>6</sub>]acetone; no binding was detected with the same guests in less polar CDCl<sub>3</sub>.<sup>34</sup> Cavitand **11** is much deeper and possesses widely extended heteroaromatic walls and a nanoscale cavity which is  $\sim 14$  Å deep and 12 Å wide.<sup>36</sup> It is probably the most sizeable open-ended container-molecule prepared to date. According to molecular modeling, such a cavity is able to accommodate up to three benzene- or chloroform-sized molecules. However, its complexing ability towards small organic guests in apolar solutions appeared to be poor. At the same time, the electron-rich interior of **11** resulted in considerable interactions with electron deficient fullerene C<sub>60</sub> in toluene solution; the association constant  $K_{\text{ass}}$  of  $900 \pm 250$  M<sup>-1</sup> ( $-\Delta G^{293} = 4.0 \pm 0.2$  kcal/mol) was determined for a 1:1 complex (Fig. 8). The open-ended nature of cavitands is clearly responsible for their modest host-guest properties. The constant flow of guests/solvent molecules in and out of the cavity readily takes place—not only through the upper neck but also through the wide holes between the aromatic walls. Competition with the multiple solvent molecules situated inside the enlarged cavity may also be the reason, and using solvent with minimal solvating ability could decrease the complexation barriers. This was actually achieved for cavitand **10**, the lipophilic interior of which was poorly solvated with rather polar [D<sub>6</sub>]acetone and therefore welcomed more lipophilic aromatic guests.<sup>34</sup> Likewise, highly hydrophobic solvents such

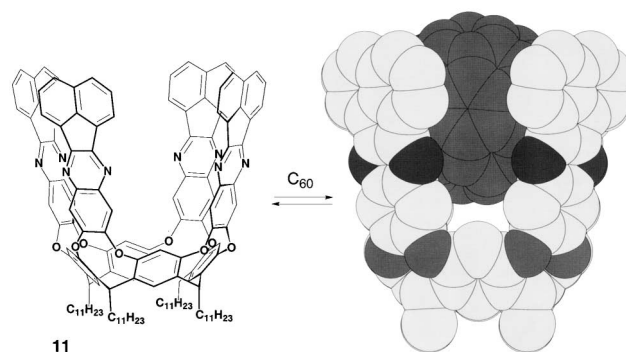


Fig. 8. Deep cavitand **11** and its 1:1 complex with C<sub>60</sub> (the energy-minimized representation).<sup>36</sup>

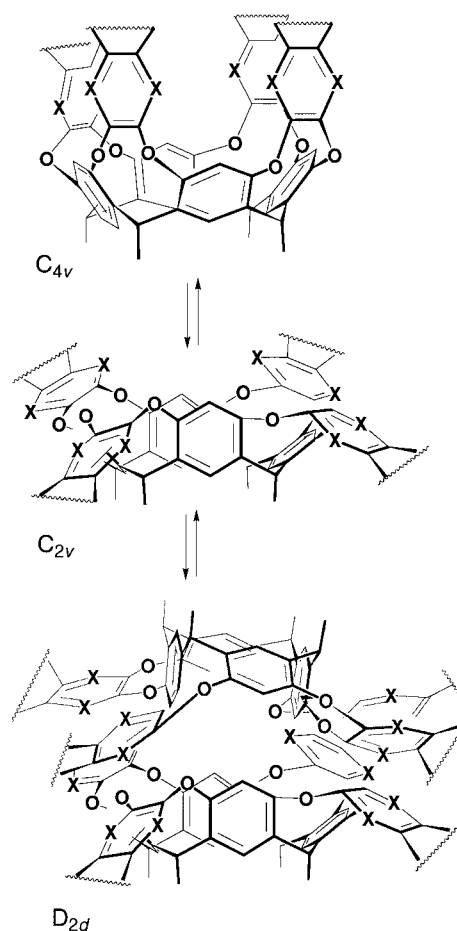


Fig. 9. Reversible “vase-kite-velcraplex” interconversions in extended cavitands.

as water can be used, as was demonstrated for complexes of nucleotides with deep cavitand **8**.<sup>32</sup> In addition, “very large” solvents can be employed which can not fit inside the cavity.<sup>37</sup> Another explanation of the weak binding capabilities of cavitands is their residual conformational flexibility. In cavitands **6–9**, the upper rim aromatic walls, attached to the calixarene skeleton, freely rotate. This is not the case for containers **10** and **11**, but they fold and unfold between C<sub>4v</sub> and C<sub>2v</sub> symmetries (Fig. 9).<sup>35,38</sup> The former has all four “walls” up and features a well-defined, vase-like shape. The latter has these walls

flipped outward in a kite-like shape. Moreover, the kite-shaped  $C_{2v}$  conformer, a *velcrand*, tends to dimerize through solvophobic interactions; the  $D_{2d}$  dimers are known as *velcra-plexes* (Fig. 9).<sup>38</sup>

The solid synthetic experience in construction of deeper cavities has been successfully used in the elaboration of much more stable nanocaviplexes, nanocarceplexes, and nanocapsules.

## 2. Self-Folding Cavitands

One of the possible ways to stabilize the rigid vase-shaped conformation in extended cavitands is to bridge their walls. Initially, this was accomplished through intramolecular hydrogen bonding. In cavitands **12**, the vicinal secondary amides at the upper rim of the molecule form a seam of head-to-tail intramolecular hydrogen bonds which results in a self-folding deepened vase with the internal dimensions of  $\sim 8 \times 10$  Å and higher kinetic stability of the caviplexes (Fig. 10).<sup>39</sup> The exchange between complexed and free guest species becomes slow on the NMR time-scale. Apparently, the circle of hydrogen bonds resists the wall's opening, thus creating a kinetic barrier to the guest escape (Fig. 11). At the same time, thermodynamic stability of the complexes with **12** remains rather low:  $-\Delta G^{298} \leq 2$  kcal/mol. The guest exchange rate in self-folding caviplexes **12** is  $k = 2 \pm 1$  s<sup>-1</sup> at 295 K.<sup>39</sup> This is faster than that observed for the completely sealed hydrogen-bonded calixarene-based capsule ( $k = 0.47 \pm 0.1$  s<sup>-1</sup>, 298 K),<sup>40</sup> or those observed for the covalently bound hemicarceplexes with sizeable guests at higher temperatures ( $k \leq 1 \times 10^{-2}$  s<sup>-1</sup>, 373 K).<sup>41</sup> The unique kinetic features of self-folding caviplexes were subsequently used in the design of larger molecular con-

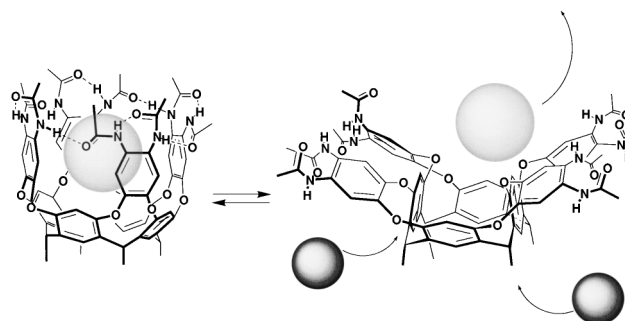
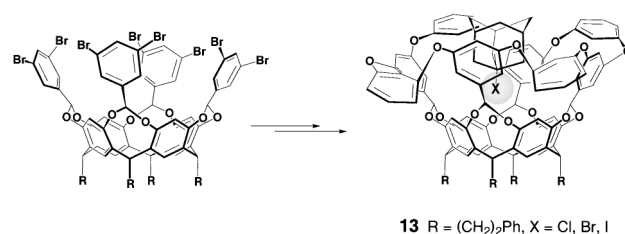
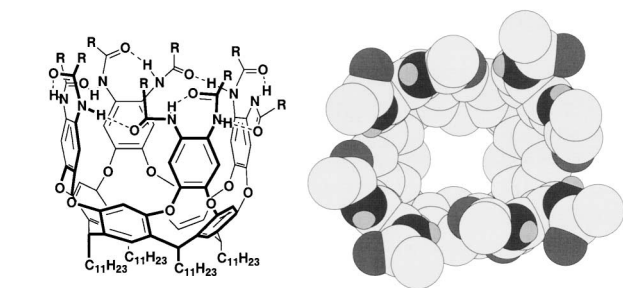


Fig. 11. Proposed mechanism for the guest-solvent exchange in self-folding cavitands.<sup>39</sup> The barrier of  $\Delta G^\ddagger \sim 17$  kcal/mol was measured for the exchange of adamantane (EX-SY; [<sup>2</sup>H<sub>10</sub>]-*p*-xylene) and the barrier of  $\Delta G^\ddagger \sim 17.5$  kcal/mol was measured for the collapse of the hydrogen bonding seam in **12** (VT <sup>1</sup>H NMR; [<sup>2</sup>H<sub>8</sub>]-toluene, [<sup>2</sup>H<sub>10</sub>]-*p*-xylene).

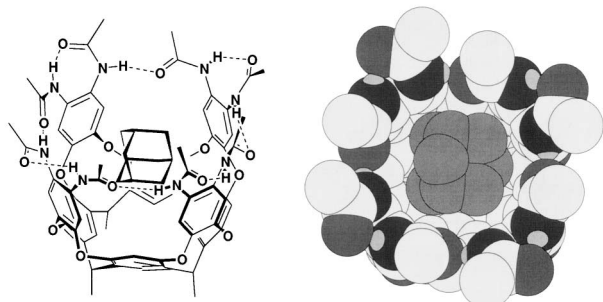


**13** R = (CH<sub>2</sub>)<sub>2</sub>Ph, X = Cl, Br, I

Fig. 12. Covalently bridged deep cavitand **13** forms kinetically stable caviplexes with 1-chloro-, 1-bromo, and 1-iodoadamantanes.<sup>47</sup>



**12** R = Alk, CH<sub>2</sub>Cl



**12-Ad**

Fig. 10. Top: self-folding cavitand **12** and its X-ray structure (top view, R = (CH<sub>2</sub>)<sub>6</sub>CH<sub>3</sub>). Bottom: energy-minimized structure of the **12**·Adamantane complex.<sup>39</sup>

tainers.<sup>42</sup> In addition, self-complementary cavitands,<sup>43</sup> cavitands with intraverted functionalities,<sup>44</sup> novel anion receptors,<sup>45</sup> and cavitand-porphyrins<sup>46</sup> were prepared. Very recently, the walls of a benzylidene bridged deep cavitand (see **9**, Fig. 7) were stitched by covalent bonds.<sup>47</sup> This resulted in a rigid, deep cavity of  $\sim 10 \times 10$  Å internal dimensions; kinetically and thermodynamically stable caviplexes **13**·Guest (Guest = 1-X-Ad; X = Cl, Br, and I) were obtained (in CDCl<sub>3</sub> and [<sup>2</sup>H<sub>8</sub>]-toluene, 298 K). The covalent seam obviously resists the wall's opening and creates a kinetic barrier for the guest escape (Fig. 12). The association constants as high as  $K_{\text{ass}} = 4393$  M<sup>-1</sup> for 1-iodoadamantane in [<sup>2</sup>H<sub>8</sub>]-toluene were obtained.<sup>47</sup> Such a large value reflects strong C-H $\cdots$ Hlg-Ad interactions with the cavity's benzal protons.

## 3. Self-Assembling Cavitands

An alternative strategy to deepen cavitands is to employ self-assembly, namely intermolecular hydrogen bonding. MacGillivray and Atwood constructed multicomponent cavitands in the solid state by co-crystallization of resorcinarene **2** (R = Me) and pyridine, 4,4'-bipyridine, 4-picoline, or 1,10-phenanthroline (Fig. 13).<sup>48</sup> While four intramolecular O-H $\cdots$ O hydrogen bonds keep the resorcinarene structure in a vase shape, four intermolecular O-H $\cdots$ N hydrogen bonds between the resorcinarene hydroxyls and four heterocyclic molecules create the enlarged cavity which is able to accommodate guest molecules. For example, co-crystallization of **2** (R = Me) and 4,4'-bipyridine from EtOH in a 1:2 ratio in the presence of ei-

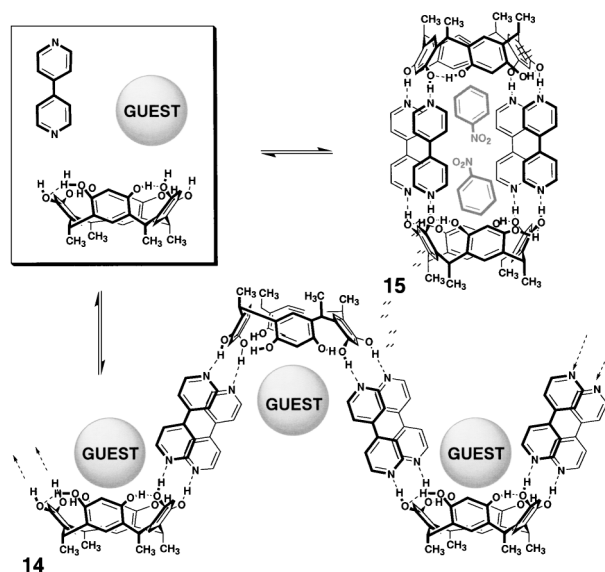


Fig. 13. Self-assembling cavitant **14** and hemicarcerand **15** (adopted from solid-state X-ray structures).<sup>48,49</sup>

ther aromatic or a polycyclic guest resulted in a one-dimensional, wave-like polymer **14**·Guest (Guest = ferrocene, 1,1'-diacetylferrocene, *p*-chlorotoluene, adamantanone, and [2.2]paracyclophane). From extensive X-ray crystallographic analysis, the polymer wavelength of  $\sim 25$  Å and the amplitude of  $\sim 19$  Å were determined. Here, guest species interact with the aromatic walls of **14** through multiple C–H $\cdots\pi$  contacts. Co-crystallization of **2** and 4,4'-bipyridine from THF or THF–CH<sub>3</sub>CN, 8:1, mixture yielded **14**·2THF and **14**·THF·CH<sub>3</sub>CN complexes, respectively. These are probably the first examples in which two guest species have been seen within an open-ended cavity. The dipole moments of the entrapped guests are aligned in an approximately anti-parallel fashion, thus maximizing attractive intermolecular electrostatic forces. Co-crystallization of resorcinarene **2** and 4,4'-bipyridine from THF–EtOH–nitrobenzene, 1:2:6 v/v, mixture resulted not in a wave-like polymer but in capsular assembly **15**.<sup>49</sup> Up to date however, this approach has not been tested in solution.

#### 4. Bis-Cavitands

In order to further enlarge the inner space and achieve cooperativity in binding, two cavitant hemispheres were attached together in a face-to-face manner with a flexible linker (Fig. 14, top). Bis-cavitands **16a,b**, which were prepared by the upper rim linking of two conformationally fixed bis(crown-3) calix[4]arenes **4**, appeared to be very strong binders of quaternary ammonium cations (Fig. 15).<sup>50</sup> While the inner space of **16a** is almost spherical, incorporation of rigid and linear ethynyl spacer between the calixarene hemispheres defines an elliptical cavity **16b** of  $\sim 7 \times 11$  Å dimensions. For such cationic guests as *N*-methylpyridinium, 2- and 4-isomeric *N*-methylpicoliniums bis-calixarenes **16a,b** showed significant binding:  $-\Delta G^{300} \sim 8$ –23 kJ/mol in CDCl<sub>3</sub> and  $-\Delta G^{300} \sim 12$ –16 kJ/mol in CDCl<sub>3</sub>–[<sup>2</sup>H<sub>3</sub>]acetonitrile, 9:1, mixture (1:1 complexation, <sup>1</sup>H NMR analysis). For monomeric bis(crown-3) calix[4]arene **4**, these values were weaker:  $\sim 11$ –15 kJ/mol and  $\sim 8$ –10 kJ/mol in CDCl<sub>3</sub> and CDCl<sub>3</sub>–[<sup>2</sup>H<sub>3</sub>]acetonitrile, 9:1,

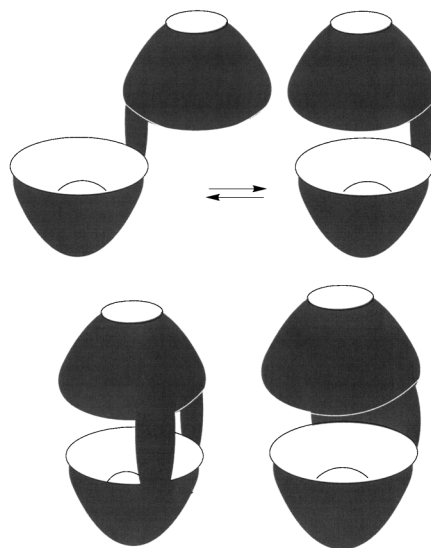


Fig. 14. Cartoon representation of bis-cavitands and clam-shell-type molecular containers.

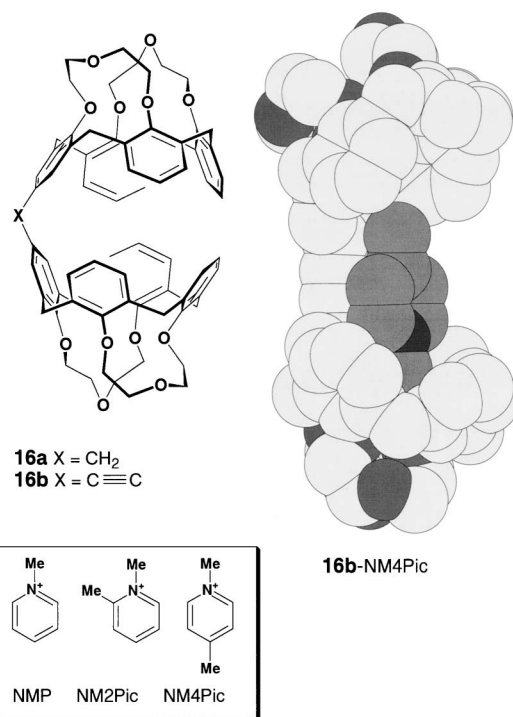


Fig. 15. Calix[4]arene based bis-cavitands **16a,b** and their cationic guests.<sup>50</sup> Right: energy-minimized structure of complex **16b**·*N*-methyl-4-picolinium.<sup>23</sup>

mixture, respectively. This comparison strongly suggests cooperative participation of both cavities in the binding event and also points at the preference of a syn-shaped conformation of the hosts upon binding. The complex formation was fast on the NMR time-scale (at ambient temperature) but the <sup>1</sup>H NMR complexation induced shifts were very significant. For example, for the **16b**·*N*-methyl-4-picolinium complex, the upfield values of  $\Delta\delta = -3.7$  and  $-3.0$  for the *N*-CH<sub>3</sub> and *p*-CH<sub>3</sub> protons, respectively, were obtained in CDCl<sub>3</sub>. These imply very

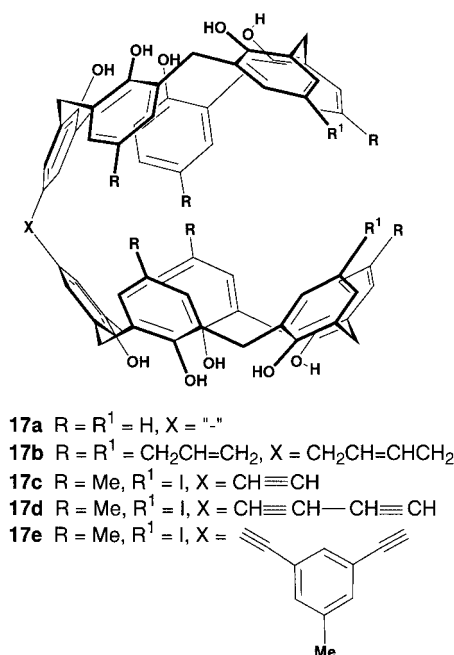


Fig. 16. Calix[5]arene based bis-cavitands **17a–e** for fullerene binding.<sup>51–53</sup>

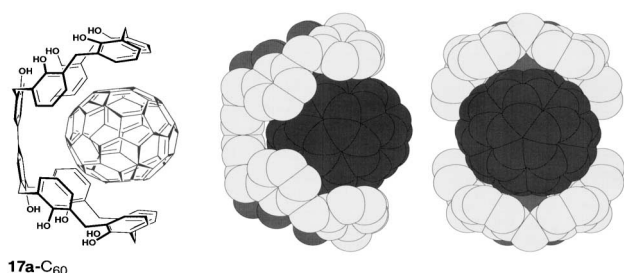


Fig. 17. Views on the X-ray structure of complex **17a**·C<sub>60</sub>.<sup>51</sup>

close contacts between the guests and the host's walls. The magnitude of CH– $\pi$  and  $\pi$ – $\pi$  interactions as well as the shielding effects are without precedent for the similar complexes of monomeric or more flexible bis-calix[4]arenes.

Bis-calix[5]arene **17a** forms 1:1 complexes with fullerenes C<sub>60</sub> and C<sub>70</sub> in CS<sub>2</sub> solution (Fig. 16).<sup>51</sup> The  $K_{\text{ass}}$  values of  $43 \pm 5$  and  $233 \pm 30 \text{ M}^{-1}$ , respectively, were determined by UV–vis spectroscopy; such numbers are higher than that for the parent calix[5]arene. Single crystal X-ray analysis of the complex **17a**·C<sub>60</sub> showed the two calixarene hemispheres in a *syn*-conformation, in a clamshell-shaped structure, inside of which C<sub>60</sub> is entrapped (Fig. 17). More extended bis-calix[5]arene **17b** (Fig. 16), bridged at the upper rim with 2-butenyl spacer and carrying *p*-allyl substituents at all other aromatic rings, binds C<sub>60</sub> and C<sub>70</sub> even more strongly: the  $K_{\text{ass}}$  values of  $1300 \pm 65$  and  $625 \pm 32 \text{ M}^{-1}$ , respectively, were determined (toluene, UV–vis spectroscopy).<sup>52</sup> Under such conditions, unsubstituted calix[5]arene binds C<sub>60</sub> and C<sub>70</sub> with the  $K_{\text{ass}}$   $30 \pm 2$  and  $51 \pm 3 \text{ M}^{-1}$ , respectively.

Fukazawa and co-workers linked two calix[5]arene hemispheres with rigid and long acetylene spacers, so the resulting molecules **17c–e** appeared to be the best binders of fullerenes

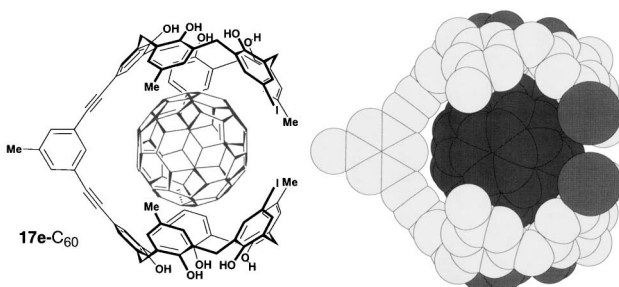


Fig. 18. Energy-minimized structure of Fukazawa's caviplex **17e**·C<sub>60</sub>.<sup>53</sup>

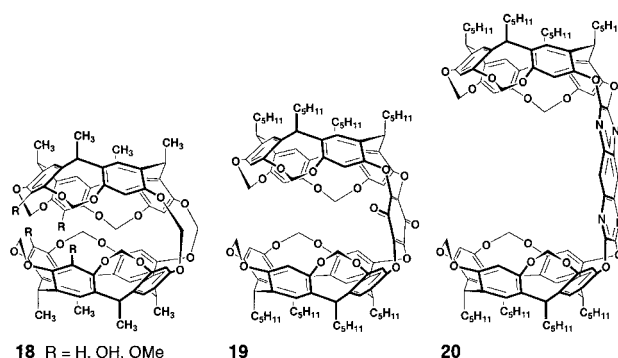


Fig. 19. Resorcinarene-based clamshell-shaped containers **18–20** of different dimensions.<sup>54,55</sup>

C<sub>60</sub> and C<sub>70</sub> in solution (toluene, benzene, CS<sub>2</sub>) to date (Fig. 16).<sup>53</sup> For example, bis-calixarene **17e** gives  $K_{\text{ass}}$  of  $(7.6 \pm 0.5) \times 10^4$  and  $(1.63 \pm 0.16) \times 10^5 \text{ M}^{-1}$  for C<sub>60</sub> and C<sub>70</sub>, respectively in toluene (Fig. 18). This is  $\geq 36$  times higher than for the C<sub>60</sub> complex of the structurally related monomeric calix[5]arenes in toluene.

## 5. Clamshell-Shaped Molecular Containers

To avoid the *syn–anti* rotation problem in bis-cavitands, more rigid linkers have been imposed (Fig. 14, bottom). For example, when two cavitand hemispheres were bridged by two short methylene linkers, the resulting C-shaped host **18** showed kinetically stable 1:1 complexes with guests like pyrazine, dioxane, and pyridine in apolar solution (Fig. 19).<sup>54</sup> Neither a structurally similar bis-cavitand connected with only one methylene linker nor a model monocavitand (see structure **3**,  $R = Me$ ,  $X = CH_2$ ) formed complexes under the same conditions.

The shape of structures **18** somewhat resembles a clamshell, and we will use this comparison elsewhere in this review. Geometrically, clamshell-shaped hosts impose more constrictive binding than cavitands and bis-cavitands, but their inner cavities are still exposed to the bulk exterior, in contrast to hemicarcerands. Unlike self-assembling capsules, their cavities are constructed through covalent bonding, and are permanent, but they are still the subject of conformational control. These features can be regulated synthetically, either by extending and modifying the walls of the hemispheres or by changing the number, geometry and conformational flexibility of the linkers. Depending on these changes, inclusion complexes of different stabilities result. Ultimately, the maximal number of

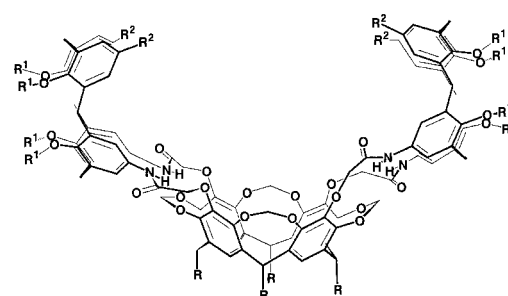


linkers will lead to hemicarcerands.

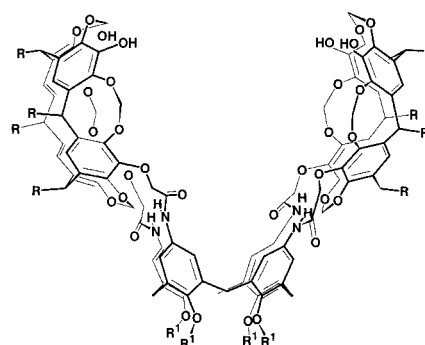
Extended clamshell-shaped container molecules were first prepared in Cram's laboratory.<sup>55</sup> Two methylene-bridged cavitands were covalently attached into the C-shaped structures **19** and **20**, connected by either fluoranil or tetraazaanthracene spacers (Fig. 19). Compound **19** was crystallized from CH<sub>2</sub>Cl<sub>2</sub>–CH<sub>3</sub>CN mixture, and, according to the single crystal X-ray analysis, there was one CH<sub>2</sub>Cl<sub>2</sub> molecule in one hemisphere and one CH<sub>3</sub>CN molecule in the other hemisphere.<sup>55a</sup> In CD<sub>2</sub>Cl<sub>2</sub> solution however, host **19** exhibited very weak complexation: such solvent molecules as C<sub>6</sub>D<sub>5</sub>NO<sub>2</sub>, C<sub>6</sub>D<sub>5</sub>CD<sub>3</sub>, *p*-CD<sub>3</sub>C<sub>6</sub>D<sub>4</sub>CD<sub>3</sub>, and CH<sub>3</sub>COCH<sub>2</sub>CH<sub>3</sub> were bound with  $K_{\text{ass}} \sim 1 \text{ M}^{-1}$ . The two concave hemispheres in **20** form an egg-shaped cavity of  $\sim 14 \text{ \AA}$  in length (X-ray).<sup>55b</sup> At the same time, not much is known yet on the binding ability of this host.

Reinholdt and co-workers reported the synthesis of more complex, large clamshell-shaped hydrophobic surfaces **21** and **22** by combination of either two calix[4]arenes and one resorcinarene or one calix[4]arene and two resorcinarenes (Fig. 20).<sup>56</sup> Four strong, intramolecular hydrogen bonds between the bridging acetamide CH<sub>2</sub>C(O)–NH and the oxygens of the cavitant acetal bridges were found to significantly rigidify the structure of these extended surfaces. These hosts bind corticosteroids, carbohydrates, nucleosides and alkaloids ( $-\Delta G^{298} = 11\text{--}16 \text{ kJ/mol}$  for 1:1 complexation) in CDCl<sub>3</sub> solution. Although the binding process was fast on the NMR time-scale, the structure of some steroid complexes was deduced by systematic <sup>1</sup>H NMR studies. Hydrogen bonding and CH– $\pi$  interactions are the main driving forces for the complexation. Such enormously extended lipophilic surfaces should be very effective in aqueous media. Moreover, they may also complex fullerenes in apolar solution with the formation of complexes similar to those with bis-cavitands **17**.

Pronounced kinetic and thermodynamic stabilities of the inclusion complexes were detected for self-folding hosts **23** and **24** of nanoscale dimensions— $10 \times 23 \text{ \AA}$  and  $\sim 800 \text{ \AA}^3$  internal volume (Figs. 21, 22).<sup>42</sup> Host **23** is flexible: the *syn*- and *anti*-



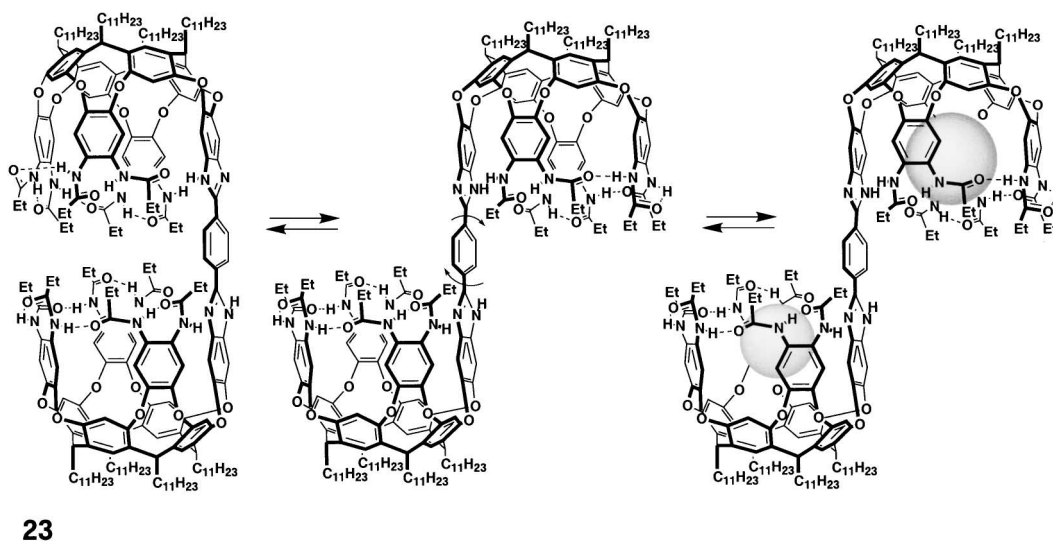
**21** R = (CH<sub>2</sub>)<sub>10</sub>CH<sub>3</sub>; R<sup>1</sup> = (CH<sub>2</sub>)<sub>2</sub>OCH<sub>2</sub>CH<sub>3</sub>;  
R<sup>2</sup> = H or R = (CH<sub>2</sub>)<sub>10</sub>CH<sub>3</sub>; R<sup>1</sup> = (CH<sub>2</sub>)<sub>2</sub>CH<sub>3</sub>;  
R<sup>2</sup> = NO<sub>2</sub>, Phth, NHC(O)CH<sub>3</sub>, *t*Bu, CN



**22** R = (CH<sub>2</sub>)<sub>10</sub>CH<sub>3</sub>; R<sup>1</sup> = (CH<sub>2</sub>)<sub>2</sub>CH<sub>3</sub>

Fig. 20. Reinholdt's extended surfaces **21** and **22**.<sup>56,57</sup>

conformers interconvert fast on the NMR time-scale. In contrast, compound **24** and its *anti*-diastereomer were easily separated by chromatography. As expected for self-folding cavitands of this type,<sup>39</sup> the complexation processes with **23** and **24** are slow on the NMR time-scale, and kinetically stable complexes form. Two deepened cavities in **23** were shown to act independently: they simultaneously complexed two different adamantyl and cyclohexyl guests, one per each cavity.<sup>42</sup>



**23**

Fig. 21. Two rotamers of unimolecular container **23** and its termolecular caviplex filled with two different guests.<sup>42</sup> Such heterocaviplexes form together with two homocaviplexes, filled with the same guest species, in a statistical ratio upon adding two different guests.

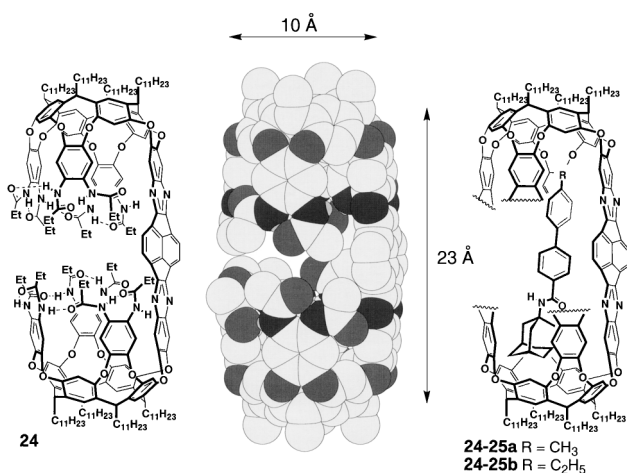


Fig. 22. Nanoscale self-folding container **24** and its energy-minimized structure.<sup>42</sup> Right: schematic depiction of complexes **24·25**. The structures were assigned by <sup>1</sup>H NMR spectroscopy and ROESY.<sup>42</sup>

Structure **24** features two cavities that are preorganized for cooperative binding (Fig. 22). Long ( $\sim 17$ – $18$  Å) and rigid guests such as diaryl-substituted adamantanes **25a,b** readily form kinetically stable 1:1 inclusion complexes, **24·25** (Fig. 22). The alkyl CH signals of the complexed **25** were observed upfield of  $\delta = 0$  and were assigned by ROESY experiments. Association constants  $K_{\text{ass}}$  up to  $500 \pm 50 \text{ M}^{-1}$  ( $-\Delta G^{295} = 3.6 \pm 0.1 \text{ kcal/mol}$ ) were calculated ( $[\text{C}_2\text{H}_8]$ toluene, <sup>1</sup>H NMR experiments). These are an order of magnitude higher than the values seen for the complexes of monomeric cavitands **12** with related adamantanes. From the ROESY experiments with complex **24·25a**, the guest exchange rate constant of  $k \sim 0.5 \pm 0.3 \text{ s}^{-1}$  at 295 K was estimated. This is considerably faster than exchange in Cram's hemicarceplexes with sizeable guests at higher temperatures ( $k \leq 1 \times 10^{-2} \text{ s}^{-1}$ ,  $\geq 373 \text{ K}$ )<sup>41</sup> but slower than that of the open-ended cavitand **12** ( $k \sim 2 \pm 1 \text{ s}^{-1}$  at 295 K).<sup>39</sup> With more flexible and/or shorter ( $< 14$  Å) adamantane guests, slow exchange between the free and complexed guest species was observed only at temperatures  $< 280 \text{ K}$  ( $[\text{C}_2\text{H}_8]$ toluene).

Recently, the synthesis and characterization of self-folding clamshell-shaped cavitand-porphyrin **26** were completed.<sup>57</sup> Host **26** features a huge unimolecular cavity containing two cavitands attached to the Zn-porphyrin wall (Fig. 23). Its dimensions,  $\sim 10 \times 25$  Å place it among the largest synthetic hosts prepared to date. The metalloporphyrin fragment introduces an additional, strong binding functionality for a number of heterocycles. As a result, not only were kinetically stable caviplaxes obtained but also the unprecedentedly high thermodynamic stability of the complexes was observed for guests able to interact with both sites of **26**—the self-folding cavities and the metalloporphyrin. A series of adamantyl- and pyridyl-containing guests of various lengths were prepared and used to determine the hosts' binding abilities in solution using UV-vis and <sup>1</sup>H NMR spectroscopy. As with containers **23** and **24**, intramolecular hydrogen bonds at the upper rims of the cavitands resist the unfolding of the inner cavities and thereby increase the energetic barrier to guest exchange. The exchange is slow

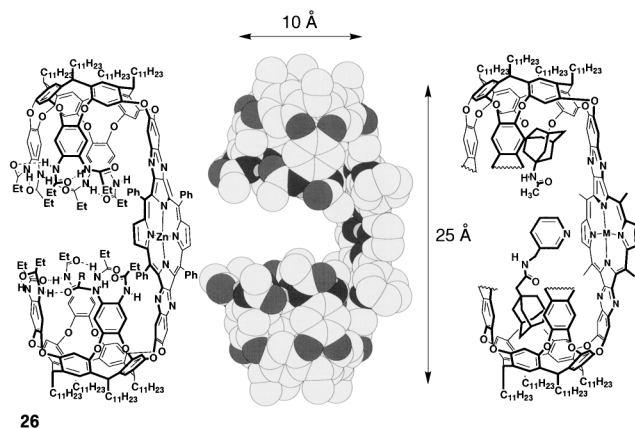
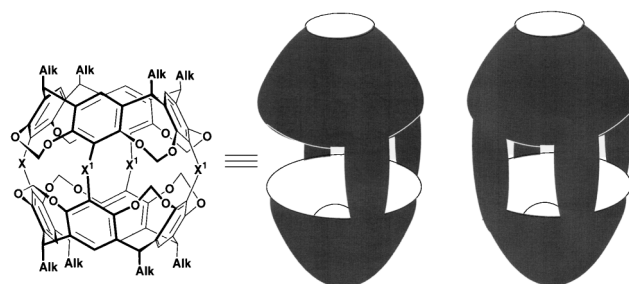


Fig. 23. Nanoscale clamshell **26** and its energy-minimized structure.<sup>57</sup> Right: schematic depiction of the ternary complex of **26** with 1-Ad-CH<sub>2</sub>C(O)NHCH<sub>2</sub>Py-3 and 1-Ad-NHC(O)CH<sub>3</sub>. The structures were assigned by <sup>1</sup>H NMR spectroscopy.<sup>57</sup>



**27a** X = "-", X' = O(CH<sub>2</sub>)<sub>n</sub>O;  
**27b** X = X' = O(CH<sub>2</sub>)<sub>n</sub>O, OCH<sub>2</sub>-arylene-CH<sub>2</sub>O, etc.

Fig. 24. Typical structures **27a,b** of Cram's hemicarcerands.

on the NMR time scale (at  $\leq 300 \text{ K}$ ). When the cavities and metalloporphyrins participate simultaneously in the binding event, very high affinities for guests are found ( $-\Delta G^{295}$  up to 10 kcal/mol in toluene), to which the porphyrin fragments contribute significantly ( $-\Delta G^{295}$  up to 6 kcal/mol). The quantitative pairwise selection of two different guests by molecular container **26** was reported (Fig. 23). The porphyrin functions also raise the possibility of metal-catalyzed reactions—alkane hydroxylations or alkene epoxidations—in these containers.

Concluding this part, we see that the unimolecular clamshell-shaped containers are relatively open and bind guests reversibly, but notably more strongly than most cavitands. This is reflected by the higher thermodynamic stabilities of their host-guest complexes. The kinetic barrier for the complex dissociation is higher as well, and the guest exchange may be slow on the NMR time scale. The maximal constrictive binding however is achieved only in sealed molecular containers such as (hemi)carcerands and capsules.

## 6. Larger Hemicarcerands

The majority of sealed nanoscale cavities are derived from hemicarcerands (see structures **27a,b**, Fig. 24). Hemicarcerands are usually divided into two structural types.<sup>10</sup> In molecules **27a** one of the bridges, connecting two hemispheres, is omitted thus opening a wider window for a guest to enter. The

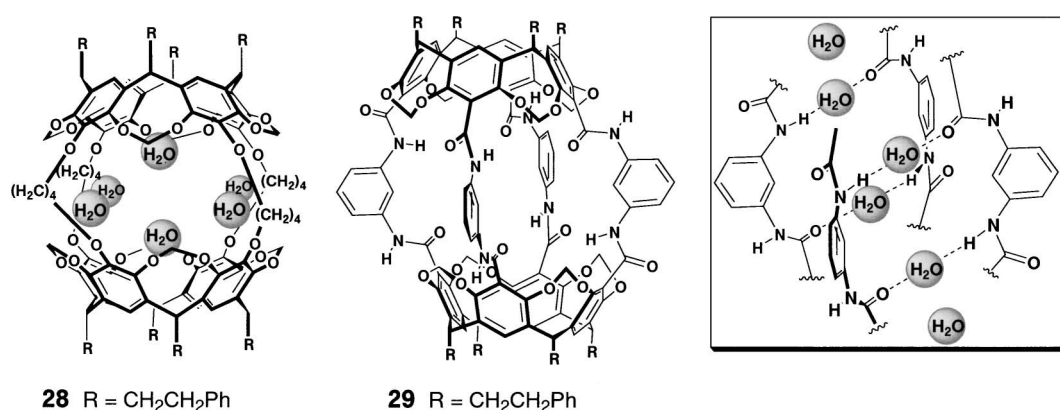


Fig. 25. Encapsulation of multiple H<sub>2</sub>O molecules by hemicarcerands **28**<sup>59</sup> and **29**.<sup>60</sup> Right: orientation of diamide linkers in hemicarcerand **29** (adopted from the X-ray structure).<sup>60</sup>

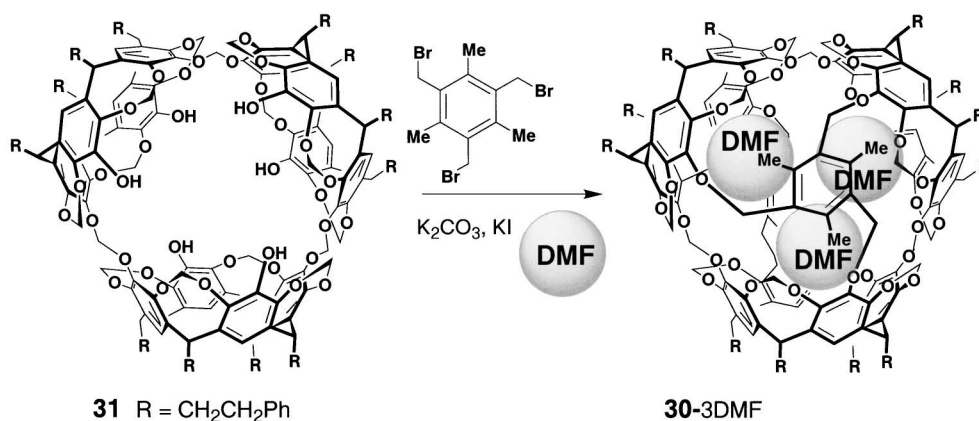


Fig. 26. Preparation of capceplex **30·3DMF**.<sup>61</sup>

other structures, **27b**, employ all four bridges but these are long and conformationally flexible, which generates temporary portals large enough to accept the guest. Hemicarceplexes are in general stable at ambient temperatures and release the entrapped guest at higher temperatures. The shielding effects of the cavity's aromatic walls cause large upfield shift ( $\Delta\delta \sim 3\text{--}5$ ) of the guest's <sup>1</sup>H NMR signals upon encapsulation. The host-guest chemistry of hemicarcerands have been thoroughly discussed in numerous reviews.<sup>3,14</sup> Here, we will only analyze the properties which arise from the nanoscale nature of the inner cavity.

One such property is a spectacular ability to entrap two or more guest molecules. We have already seen this for self-assembled caviplaxes **14·2THF** and **14·THF·CH<sub>3</sub>CN**<sup>48</sup> as well as for clamshell-shaped caviplaxes **19**<sup>55</sup> and **23**.<sup>42</sup> Already at the early stage of the carcerand research, Cram and co-workers isolated and characterized (<sup>1</sup>H NMR spectroscopy; DCI mass spectrometry) carceplexes with two CH<sub>3</sub>OH and two CH<sub>3</sub>CN molecules inside.<sup>58</sup> The larger inner size, which still maintains high kinetic stability of (hemi)carceplexes, offers more examples. Thus, hemicarcerand **28** crystallizes with six H<sub>2</sub>O molecules entrapped within its interior (Fig. 25).<sup>59</sup> The H<sub>2</sub>O molecules are hydrogen bonded to one another and also to the host's walls. This arrangement is roughly octahedral and complementary to the inner shape of **28**. The O...O distances and the

O...O...O bond angles of the encapsulated H<sub>2</sub>O are comparable with the crystallographic values of ordinary ice. Octaamide hemicarcerand **29** also entraps six H<sub>2</sub>O molecules (Fig. 25).<sup>60</sup> In the solid state structure of hemicarceplex **29·6H<sub>2</sub>O**, each of eight amides is anti-periplanar and each of the *m*-phenylenediamide fragments contains one inwardly- and one outwardly-directed carbonyl. The four out of six encapsulated H<sub>2</sub>O molecules form a square held by four C(O)N-H...OH<sub>2</sub> and four HN-C=O...HOH hydrogen bonds. The two remaining H<sub>2</sub>O molecules occupy the cavitated hemispheres.

While the original methylene-bridged carcerands (see for example, **27b**, X = X' = OCH<sub>2</sub>O) usually entrap just one DMF-sized molecule, host **30** was shown to encapsulate three DMF molecules (Fig. 26). Giant carceplex **30·3DMF** was prepared from trimer **31** and 1,3,5-tris(bromomethyl)-2,4,6-trimethylbenzene.<sup>61</sup> The complex is effectively sealed: no DMF was lost even upon heating in nitrobenzene at 160 °C for 6 hours. Enlarging the cavity's portals often leads towards more flexible hemicarcerands, which in turn decreases the kinetic stability of the hemicarceplexes.<sup>3,14</sup> To avoid this, larger container-molecules possessing more rigid portals were prepared. Hemicarcerands **32**<sup>62</sup> and **33**<sup>63</sup> were combined from two cavitand hemispheres and four relatively rigid *m*-CH=NC<sub>6</sub>H<sub>4</sub>N=CH or OCH<sub>2</sub>C≡C-C≡CCCH<sub>2</sub>O walls; they possess huge, twenty eight-, and thirty-membered portals, respectively (Fig. 27).

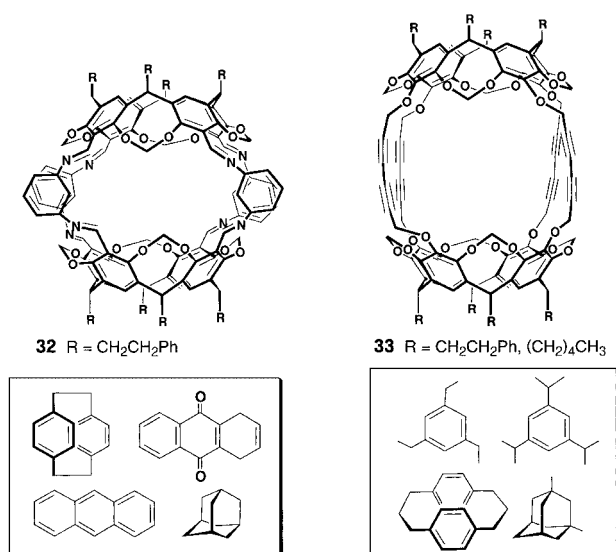


Fig. 27. Large hemicarcerands **32**<sup>62</sup> and **33**<sup>63</sup> and their guests.

When heated with such large ( $\sim 3 \times 9 \text{ \AA}$ ) guests as [2.2]paracyclophane, anthracene, and 9,10-anthraquinone, host **32** produced stable 1:1 hemicarceplexes (<sup>1</sup>H NMR, FAB MS, elemental analyses). Tripiperidylphosphine oxide was employed as a solvent, which is too bulky to enter the cavity **32**. The kinetic stability of the hemicarceplexes was determined by Variable Temperature <sup>1</sup>H NMR spectroscopy (CDCl<sub>2</sub>CDCl<sub>2</sub> and/or CDCl<sub>3</sub>, 25–134 °C) and, for larger guests, is in this order: **32**·[2.2]paracyclophane > **32**·adamantane > **32**·9,10-anthraquinone > **32**·anthracene. At the same time, the portals in **32** were still narrow enough to safely retain smaller guests such as ferrocene and adamantane ( $\sim 4.5 \text{ \AA}$ ). The activation barriers ( $E_a$ ) of decomplexation are high: for example, for **32**·adamantane  $E_a \sim 28 \text{ kcal/mol}$ .<sup>62</sup> Portals of hemicarcerand **33** contain a minimum of hydrogens to block the guest exchange. At the same time, twist of the diacetylene linkers can significantly decrease the cavity size and close the portals. When used as solvents, 1,3,5-triethylbenzene, 1,3,5-tri-*i*-propylbenzene, and 1,3-dimethyladamantane produced 1:1 hemicarceplexes with **33** upon heating. Very bulky 1,3,5-tri-*t*-butylbenzene was not able to enter the portals at all. It was used as a solvent in which 1:1 hemicarceplexes of **33** were produced with nine different [*m.n*]paracyclophanes. The largest encapsulated guest was [3.3]paracyclophane. The half-lives for decomplexation with these large guests were extremely high—1608 hours for **33**·1,3,5-tri-*i*-propylbenzene and 960 hours for **33**·1,3,5-triethylbenzene (CDCl<sub>3</sub>, 25 °C). On the other hand, the portals could not retain smaller ferrocene and 9,10-anthraquinone.<sup>63</sup>

In challenging efforts to entrap even larger guests, much more sizeable hemicarcerands **34–36** were prepared (Figs. 28 and 29). To our knowledge, they possess the largest covalently sealed cavities synthesized to date. Host **34** has portals and interiors large enough for fullerene C<sub>60</sub> ( $\sim 7 \text{ \AA}$  diameter) and tetraphenylporphyrin ( $\sim 12 \times 17 \text{ \AA}$ ) to enter (Fig. 28).<sup>64</sup> The **34**·metalloporphyrin complex may be interesting as an oxidation catalyst stabilized by the cavity. Figure 28 represents mo-

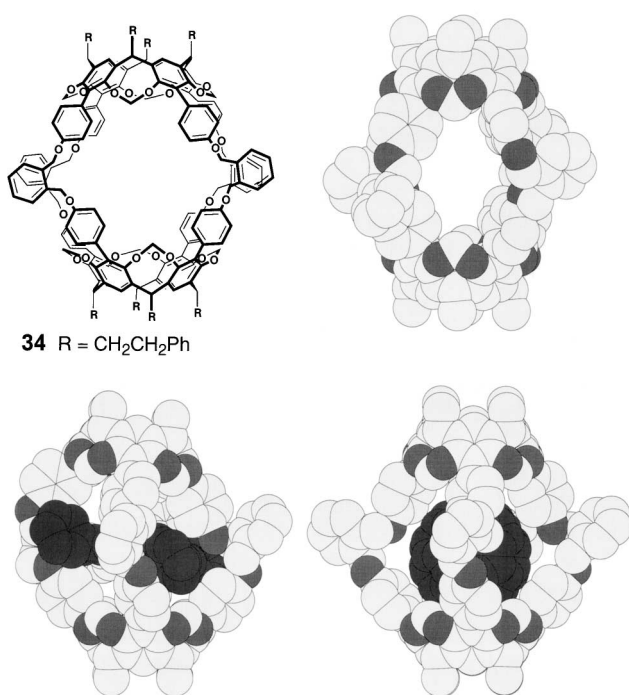


Fig. 28. Top: nanoscale hemicarcerand **34** and its X-ray structure.<sup>64</sup> Bottom: energy-minimized structure<sup>23</sup> of complexes **34**·tetraphenylporphyrin and **34**·C<sub>60</sub>. The preliminary MM2 calculations<sup>64</sup> suggested that the activation barrier for the **34**·C<sub>60</sub> decomplexation is very high:  $E_a \sim 56 \text{ kcal/mol}$ .

lecular models of such potential complexes. At the same time, all experimental attempts to encapsulate these guests failed, even at higher temperatures (CDCl<sub>2</sub>CDCl<sub>2</sub>, 130 °C, 20 h for fullerene C<sub>60</sub>, and CDCl<sub>3</sub>, 60 °C, 3 days for porphyrin).<sup>64</sup> Structurally similar hemicarcerand **35** (Fig. 29) was prepared recently from two benzylidene-bridged deep cavitands **9** ( $R = \text{CH}_2\text{OH}$ ) and CH<sub>2</sub>BrCl (*t*-BuOK, DMSO).<sup>65</sup> From the single crystal X-ray analysis, the inner cavity dimensions of  $15 \times 19 \text{ \AA}$  and the portals of  $\sim 9.5 \times 11.5 \text{ \AA}$  were determined, but no encapsulation studies have been thus far reported.

Holand **36** was prepared by multistep combination of two calix[4]arenes and two resorcinarene-based cavitands, following the strategy applicable for the previously discussed hosts **21** and **22**.<sup>66</sup> By definition, *holand* is a receptor molecule with a permanent hole. The axes of **36** are  $\sim 15 \times 20 \text{ \AA}$  and the estimated internal volume is  $\sim 1000 \text{ \AA}^3$  (Fig. 29). Holand **36** is much more rigid than even hemicarcerands **32–35**. Not only the intrinsic rigidity of its calixarene components and of the amide bridges is responsible, but also eight intramolecular hydrogen bonds between the bridging acetamide CH<sub>2</sub>C(O)–NH and the oxygens of the cavitand acetal bridges helps to rigidify the structure and significantly reduce the portal's size and flexibility. By our own estimation,<sup>23</sup> the portals are egg-shaped and of  $\sim 6 \times 15 \text{ \AA}$  dimensions. According to the extensive computer modeling,<sup>66</sup> tetraphenylporphyrin, phthalocyanine, medium-sized dibenzocrown ethers, and steroids would nicely fit within the interior of **36**, but the complexation experiments have thus far met with little success.

In general, the hemicarceplex stability is provided through a

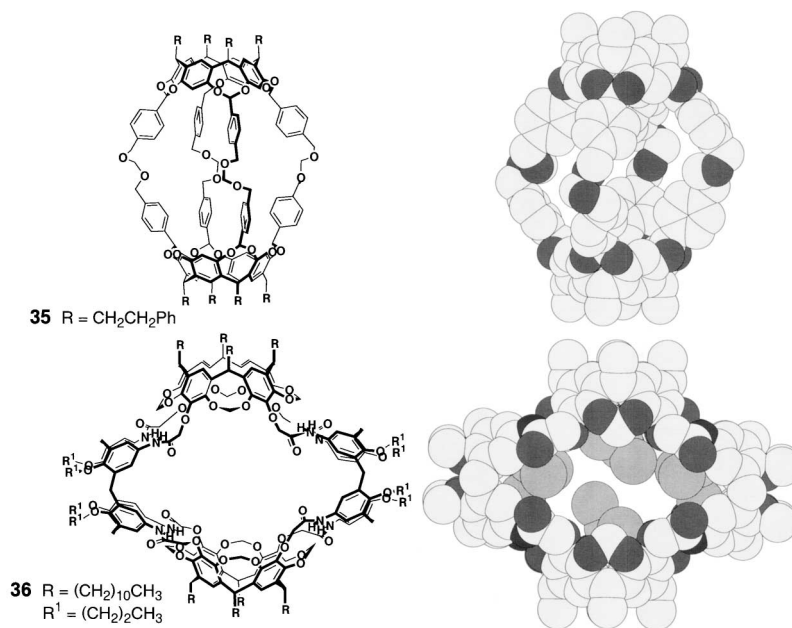


Fig. 29. Nanoscale molecular containers. Top: hemicarcerand **35** and its X-ray structure.<sup>65</sup> Bottom: holand **36**<sup>66</sup> and the energy-minimized representation<sup>23</sup> of complex **36**·4CHCl<sub>3</sub>.

constrictive binding (see the introduction).<sup>22</sup> Both the cavity and the portal's dimensions and their conformational rigidity have a very significant influence on the association and dissociation activation energies. As mentioned earlier, enlarging the cavity easily leads to the host's higher flexibility; the two hemispheres often undergo twists and turns with respect to each other, as is seen in the X-ray structures of Cram's larger hemicarcerands.<sup>60,64</sup> The kinetic stability of the complexes decreases when the portals are widely open allowing the guest to escape easily. At the same time, twists and turns of the linkers can significantly decrease the cavity size and close the portals after the complex is formed. Very rigid and preorganized portals prevent the guest from entering.

Not only the guest's size but also its shape is crucial. Generally, occupancy factors, or packing coefficients, of molecule-within-molecule complexes in solution are of a  $55 \pm 9\%$  value.<sup>67</sup> Competition with the multiple solvent molecules situated inside the cavity may be one important reason to block the guests entering. Thus, extensive molecular modeling with holand **36** in a solvent box strongly suggests that four CHCl<sub>3</sub> or THF molecules comfortably fit inside<sup>66</sup> and do not exchange with each other or with the solvent molecules from the bulk solution. Due to such strong solvation, it may be difficult for other guests to enter the cavity. Similarly to Cram's hemicarcerands, it was proposed to diminish solvation of holand **36** by using a solvent that is too bulky to fit inside or at least to enter its portals.

Indeed, using a solvent with minimal solvating ability can decrease the association barriers. For the cases with hemicarcerands **32–36**, this must be a "very large" solvent. However, the commercial availability of such solvents is limited. Alternatively, highly hydrophobic solvents such as water can be used. Recent success with water-soluble cavitands and a hemicarcerand that are highly lipophilic in their interior offers the examples: kinetically and thermodynamically stable complex-

es readily formed in these cases with a number of sizeable organic guests.<sup>68</sup>

On the other hand, the stability of the encapsulation complexes may be increased through the introduction of additional binding sites within the cavity's interior. It has been demonstrated that, even in widely open cyclophane-like structures, strong guest binding can be achieved when Lewis acidic binding centers,<sup>69</sup> metalloporphyrin fragments<sup>70</sup> or hydrogen bonding sites are properly attached to the receptor's concave interior.<sup>71</sup> Finally, structural elimination of one of the linkers in larger hemicarcerands may open the wider gate for the nano-sized guests. This would transform hemicarcerands into clam-shell-type containers (see Section 5).

## 7. Dynamic Features of Hemicarcerands

Chemical manipulations with already preformed hemicarcerands may as well change their host-guest properties. Recently, Stoddart and co-workers proposed<sup>72</sup> to use thermodynamically controlled covalent bond formation—dynamic covalent chemistry—for regulation of the encapsulation process in large hemicarceplexes. They showed that, due to the reversible nature of the imine  $\text{HC}=\text{N}$  bond in hemicarcerands **32**, its *m*-phenylenediimine linkers can be cleanly replaced by other, structurally related arylene diimine substituents.<sup>72</sup> This was demonstrated through the exchange of 5-[C(O)OCH<sub>2</sub>CH<sub>2</sub>-OCH<sub>2</sub>CH<sub>2</sub>OCH<sub>3</sub>]-1,3-CH=NC<sub>6</sub>H<sub>4</sub>N=CH to 1,3-CH=NC<sub>6</sub>H<sub>4</sub>N=CH fragments in molecule **32**. In a stepwise process, the bridges open, close and are being replaced at room temperature in CDCl<sub>3</sub>-CF<sub>3</sub>COOH, 99:1. When a ferrocene molecule is incarcerated inside **32**, the imine exchange and/or hydrolysis allows the guest to escape (Fig. 30). This impressive finding offers a novel mechanism for the guest exchange in hemicarceplexes. Indeed, dynamic covalent chemistry has already utilized such commonly useful reactions as acetal, ester, hydrazone, disulfide, and oxime bond formation. These may be ap-

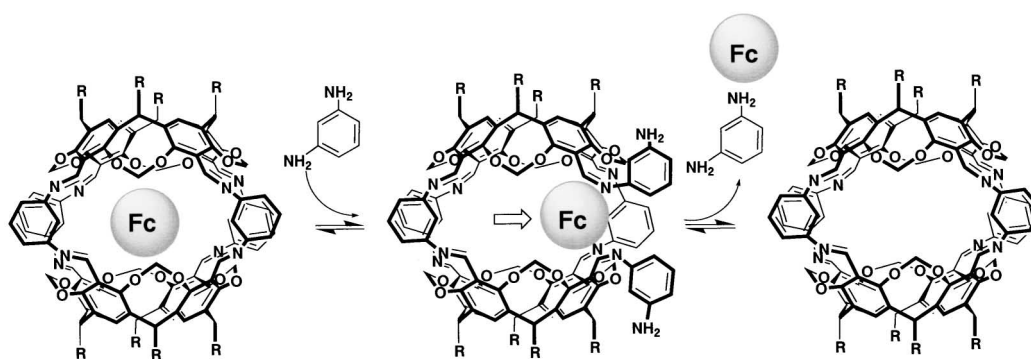


Fig. 30. Guest replacement in hemicarceplex **32**·ferrocene occurs via breaking and remaking of dynamic covalent bonds.<sup>72</sup>

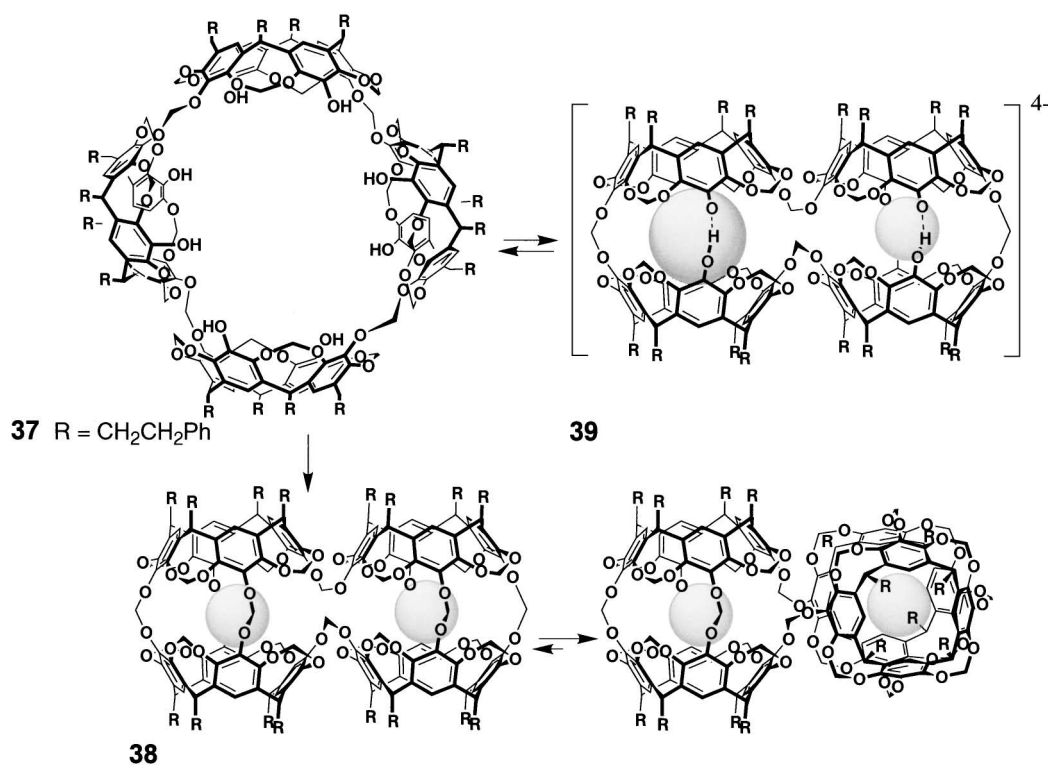


Fig. 31. Sherman's bis-carcerand **38**<sup>73</sup> and self-assembling bis-capsule **39**.<sup>74</sup>

plied in the shell-closure of (hemi)carcerands and/or in the formation of (hemi)carceplexes, without either hemicarceplex or initial hemicarcerand falling apart into its individual components. Moreover, dynamic covalent chemistry may, in principle, be also employed in the construction of deep cavitands and clamshell-shaped nanoscale hosts.

Macrocycle **37** consists of four methylene-bridged cavitands connected with  $\text{OCH}_2\text{O}$  linkers; its inner cavity is large enough to accommodate fullerenes.<sup>73</sup> However, when submitted to the reaction with  $\text{CH}_2\text{BrCl}$ ,  $\text{K}_2\text{CO}_3$  and *N*-methylpyrrolidinone in the presence of pyrazine as a template, it folds into two cavities, around two template molecules, and affords bis-carceplex **38** (Fig. 31).<sup>73</sup> The reaction proceeds in 74% yield, and the pyrazine guests do not escape even upon reflux at 214 °C in 1,2,4-trichlorobenzene for 84 hours. When ~4 equivalents of 1,8-diazabicyclo[5.4.0]undec-7-ene (DBU) was added to the solution of **37** in  $\text{CDCl}_3$ , four charged  $\text{O}^- \cdots \text{H}-\text{O}$  hydrogen

bonds formed to exclusively produce bis-capsule **39** filled with two  $\text{CDCl}_3$  molecules.<sup>74</sup> Similarly, two pyrazines or two MeOAc molecules were encapsulated. Half-empty, 1:1 host-to-guest complex was not detected. When mixtures of two guests were employed, heterobis-capsules were obtained. In those, the  $^1\text{H}$  NMR chemical shifts of the encapsulated MeOAc appeared to be sensitive towards the neighboring guest species; the  $\Delta\delta = \delta(\mathbf{39} \cdot \text{MeOAc} \cdot \text{Guest}) - \delta(\mathbf{39} \cdot 2\text{MeOAc})$  magnitude ranges from  $\Delta\delta = 0.05$  to 0.16. Obviously, such communication between the guests occurs through two aromatic walls, via conformational fluctuations.<sup>74</sup>

Large homooxalix[3]arene-based hemicarcerand **40A**, one of the calix hemispheres of which possesses OMe substituents and the other  $\text{OCH}_2\text{C}(\text{O})\text{Et}_2$  substituents, exists in equilibrium with its "self-threaded rotaxane" **40B** (Fig. 32).<sup>75</sup> The two forms interconvert by inverting aromatic rings of the OMe-substituted hemisphere but such a process is prohibited

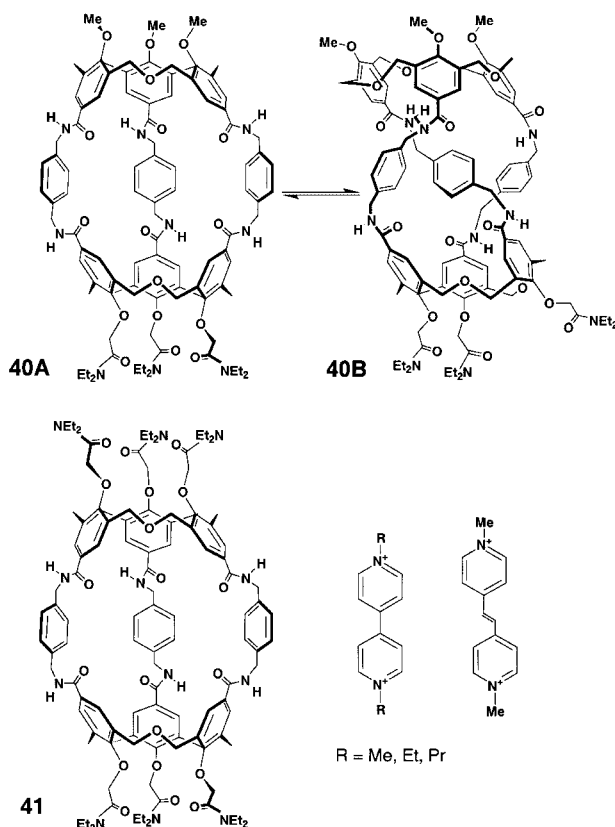


Fig. 32. Shinkai's dynamic hemicarcerands **40** and **41** and their guests.<sup>75</sup>

for bulkier  $\text{OCH}_2\text{C}(\text{O})\text{NEt}_2$  substituents. The two conformers **40A** and **40B** exist in a slow exchange on the NMR time scale in the 0–120 °C temperature range ( $\text{Cl}_2\text{CDCDCl}_2$ ). For instance, the rotaxane/capsule ratio decreased with the temperature increase—from 3.8 to 1.8 at 0 °C to 120 °C. In contrast, symmetrical hemicarcerand **41** is conformationally rigid and readily exhibits complexation of large organic cations—1,1'-dimethyl-4,4'-bipyridinium (methyl viologen,  $K_{\text{ass}} = 430 \text{ M}^{-1}$ ), 1,1'-diethyl-4,4'-bipyridinium (ethyl viologen,  $K_{\text{ass}} = 116 \text{ M}^{-1}$ ), 1,1'-dipropyl-4,4'-bipyridinium (propyl viologen,  $K_{\text{ass}} = 97 \text{ M}^{-1}$ ), and 1,2-bis(1-methyl-4-pyridinio)ethylene ( $K_{\text{ass}} = 210 \text{ M}^{-1}$ ) ( $\text{Cl}_2\text{CDCDCl}_2$ - $\text{CD}_3\text{OD}$ , 98:2 v/v). Addition of **41** to a solution of the guest caused clear upfield shifts of the guest's *N*-alkyl and CH aromatics  $^1\text{H}$  NMR signals, which suggests encapsulation. In the series, propyl viologen is bound most weakly, perhaps representing the length limits of the inner cavity. Much weaker binding was detected for the model, monomeric homooxalix[3]arene. No binding studies have been reported thus far with flexible hemicarcerand **40**.<sup>75</sup> The described phenomena can be very useful in establishing a switchable control of complexation behavior of nanoscale containers in solution. The uptake and release of guests must involve the folding and unfolding of the host(s), but these motions are reversible and can be strongly influenced by solvent size and polarity, and also by temperature. Thus, some conditions could be found to “turn off” the collapsing system. Moreover, the right guest may act as a template and shift the equilibrium towards the “empty” cavity, which is able to encapsulate. On the other hand, the guest can be driven away if the conditions

are changed in favor of hydrophobic collapse.

## 8. Self-Assembling Nanocapsules

The dynamic properties of nanoscale cavities reach their extreme in self-assembling capsules. Self-assembly represents an alternative, very popular way to construct nanocavities and their host–guest complexes.<sup>11,12</sup> Calixarenes, in particular, have had a great impact in the history of this subject.<sup>76</sup> With appropriate curvature and carefully engineered positioning of interacting sites, calixarene-based self-assembling systems generate capsules. Capsules have been organized through hydrogen bonding and metal–ligand interactions. Hydrogen bonding is highly directional and specific. Metal–ligand attractive forces are much stronger, and metal-induced assemblies are more robust. Nevertheless, their strength can be controlled by solvent polarity and pH. They can be charged and redox-active. Here we only discuss construction and properties of self-assembling nanocapsules. Similarly to covalently constructed hemicarcerands, the capsule's complex stability is influenced mostly by energetic barriers for the guest exchange. At the same time, the encapsulation processes here are easier to control, since the capsule's formation-dissipation is under equilibrium conditions. Encapsulation is largely determined by the host and guest volumes, and Rebek's occupancy factors ( $55 \pm 9\%$ ) for molecule-within-molecule complexes in solution are well-applicable in this case.<sup>67</sup> Multiple solvent molecules situated inside the nanocapsule may be replaced by the best-fitting guest; often this is an entropically favorable process. Alternatively, the use of very bulky solvents also facilitates the encapsulation. At the same time, as self-assembling cavities emerge larger and larger it becomes increasingly difficult to find such a solvent. Early generations of self-assembling capsules include Rebek's sportsballs<sup>17</sup> and calix[4]arene tetraurea dimers **42** (Fig. 33).<sup>77</sup> These are quite small, with 50–250 Å<sup>3</sup> of internal volume, and in most of the cases entrap a single guest-molecule of moderate dimensions.<sup>67,78</sup> More peculiar encapsulation phenomena emerge in nanocapsules. Deepened calix[4]arene tetraurea **6** ( $\text{R} = \text{CH}_2\text{C}(\text{O})\text{NEt}_2$ ,  $\text{R}^1 = p\text{-[NHC}(\text{O})\text{NH}-\text{C}_6\text{H}_4-p\text{-(CH}_2)_6\text{CH}_3]$ ) reversibly dimerizes into large egg-shaped cavity **43** of  $\sim 400 \text{ Å}^3$  internal volume ( $^1\text{H}$  NMR spectroscopy, ESI mass spectrometry).<sup>79</sup> This is twice as large as the original calix[4]arene tetraurea capsules **42** ( $\sim 200 \text{ Å}^3$ ).<sup>77</sup> The self-complementary urea NH and C=O groups at the upper rim assemble in a head-to-tail fashion, and capsule **43** is held together by a seam of sixteen, intermolecular  $\text{C}=\text{O} \cdots \text{H}-\text{N}$  hydrogen bonds around the equator (Fig. 33). Due to the large holes/portals, the solvent/guest exchange in and out of the cavities **43** is fast on the NMR time scale at ambient temperatures. Nevertheless, dimer **43** readily complexes sizeable *p*-substituted *N*-methylpyridinium derivatives (substituent = *i*-Pr, Ph,  $\text{CH}=\text{CH}-\text{C}_6\text{H}_4-\text{NMe}_2$ -*p*) which are up to 14 Å long. From the NMR titration experiments in  $\text{CD}_2\text{Cl}_2$ , the  $K_{\text{ass}}$  values between  $5.6 \times 10^3$  and  $1.9 \times 10^5 \text{ M}^{-1}$  were determined, which correspond to  $-\Delta G^{295} = 5.0\text{--}7.1 \text{ kcal/mol}$ . Encapsulation of a deep-red dye, *trans*-4-[4-(dimethylamino)styryl]-1-methylpyridinium iodide, resulted in a hypsochromic UV–vis shift from  $\lambda_{\text{max}} = 518$  to  $\lambda_{\text{max}} = 497$ .

Self-complementary cyclic tetraimides built on the resorcinarene platform, dimerize through hydrogen bonding to af-

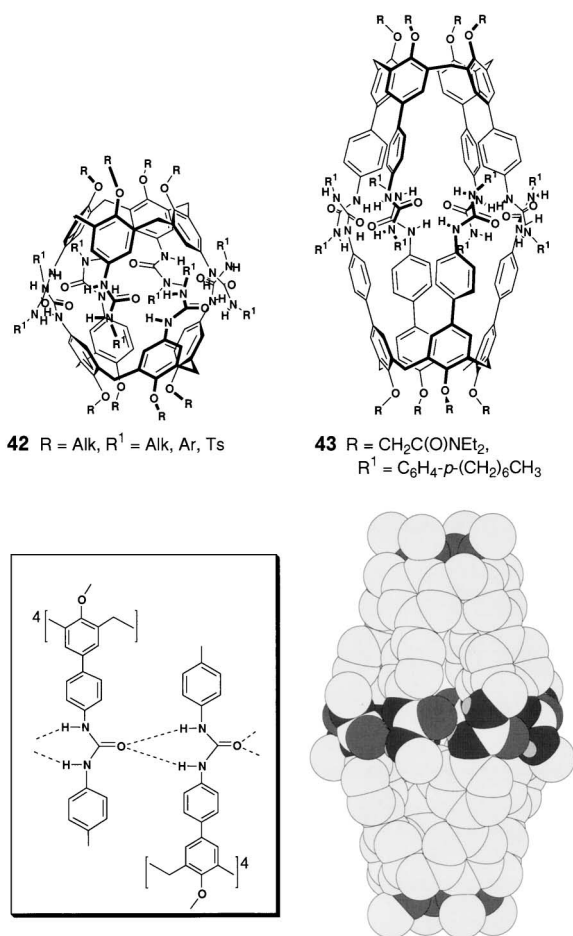


Fig. 33. Top: self-assembling calix[4]arene capsules **42**<sup>77</sup> and **43**.<sup>79</sup> Bottom: depiction of intermolecular hydrogen bonding in dimer **43** (left) and its energy-minimized structure.<sup>79</sup>

ford cylindrical capsule **44**. Its estimated internal volume is 460 Å<sup>3</sup> and the internal dimensions are 6 × 15 Å (Fig. 34).<sup>80</sup> In contrast to capsule **43**, cavity **44** is built in such a way that its inner space is well protected from the bulk solution and the portal's dimensions are minimal. In [2H<sub>12</sub>]mesitylene which is too bulky to fit inside, capsule **44** disassembles, but addition of some benzene or toluene immediately results in complex **44**·2Guest; two benzene or toluene molecules were quantitatively encapsulated inside **44** (<sup>1</sup>H NMR spectroscopy). The complexes are kinetically stable at ambient temperatures, and all the encapsulation processes with **44** are slow on the NMR time-scale. When both benzene and *p*-xylene were added in a 1:1 ratio to a [2H<sub>12</sub>]mesitylene solution of **44**, an unsymmetrically filled capsule formed predominantly. Such pairwise selection of the guests was also observed for benzene with *p*-trifluoromethyltoluene, *p*-chlorotoluene, 2,5-lutidine, and *p*-methylbenzyl alcohol to give new species with one of each guest inside.<sup>81</sup> Moreover, capsule **44** exhibits complexation of smaller hydrogen bonded aggregates—2-pyridone/2-hydroxypyridine dimer, benzamide and benzoic acid dimers, and *trans*-1,2-cyclohexanediol dimers.<sup>82</sup> When equal amounts of α-, β-, and γ-picolines were added to a [2H<sub>12</sub>]mesitylene solution of **44**, in addition to the corresponding homocapsules, nonsymmetrical-

ly filled heterocapsules were also formed and they were identified by <sup>1</sup>H NMR spectroscopy.<sup>83</sup>

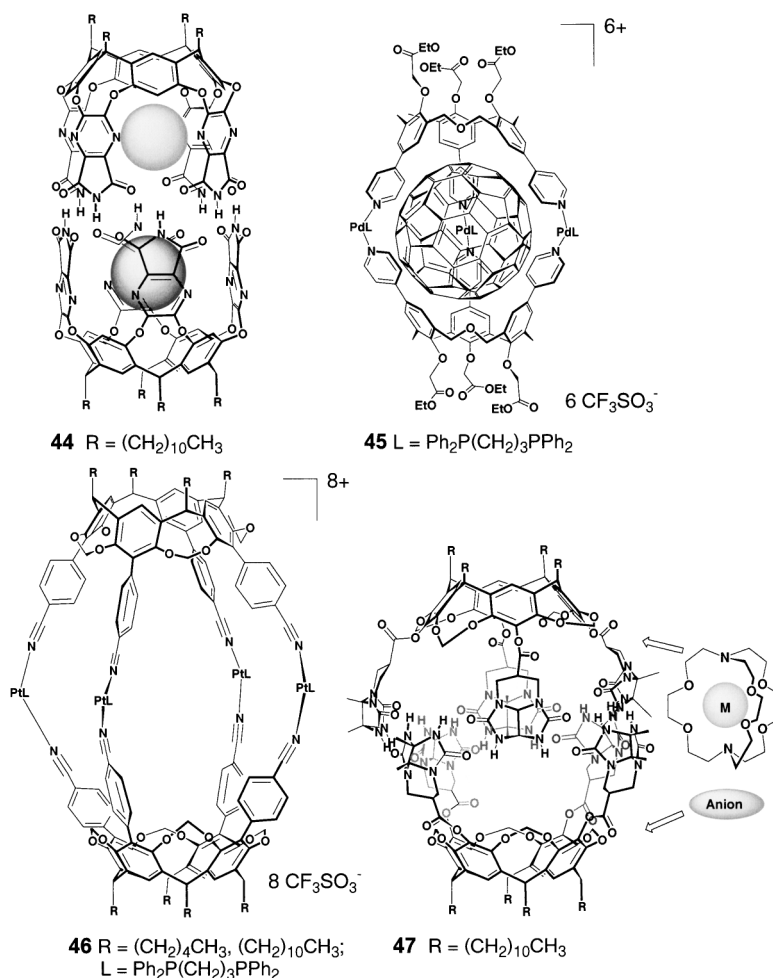
Capsule **44** was used to entrap such important chemical reagents as dicyclohexylcarbodiimide (DCC) and dibenzoyl peroxide (DBPO). Chemical stability of DCC and DBPO complexed inside capsule **44** was greatly improved. For example, inside the capsule DBPO is stable for at least 3 days at 70 °C in [2H<sub>12</sub>]mesitylene solution, while in the absence of **44** it decomposes within 3 hours under those conditions.<sup>80</sup> Due to the reversible nature of the hydrogen bonds stitching **44**, the encapsulated DCC and DBPO can be released by competitive guest-molecules or polar solvents in a time-scale from seconds to days.<sup>80</sup>

When mixed with three equivalents of Pd(II)(Ph<sub>2</sub>PCH<sub>2</sub>CH<sub>2</sub>CH<sub>2</sub>PPh<sub>2</sub>)(OTf)<sub>2</sub> in CH<sub>2</sub>Cl<sub>2</sub>, two *p*-pyridyl substituted homooxacalix[3]arenes readily afford capsule **45** (Fig. 34).<sup>84</sup> Dimer **45** forms a kinetically stable 1:1 complex with fullerene C<sub>60</sub> (<sup>1</sup>H and <sup>13</sup>C NMR spectroscopy, Cl<sub>2</sub>CDCDCl<sub>2</sub>). The association constants *K*<sub>ass</sub> of 39 M<sup>-1</sup> at 30 °C and 54 M<sup>-1</sup> at 60 °C were obtained. Complexation of Li<sup>+</sup> cation at the calixarene lower rims induces their more flattened conformation and significantly improves the *K*<sub>ass</sub> value to 2100 M<sup>-1</sup> (30 °C).<sup>85</sup> Analogously, the pyridyl-Pd(II) interactions were employed in the construction of *p*-pyridyl-calix[4]arene-based capsules.<sup>86</sup> Noteworthy, only conformationally rigid bis-(crown-3) derivatives appeared to be useful for this purpose, while assemblies based on the more flexible tetrakis-*O*-alkylated calix[4]arene resulted in ill-defined oligomers. In a similar fashion, Dalcanele and co-workers constructed much larger dimer **46** (Fig. 34). It self-assembled at room temperature from two deepened tetracyanocavitands **7** (R<sup>1</sup> = CN) and four equivalents of Pt(II)(Ph<sub>2</sub>PCH<sub>2</sub>CH<sub>2</sub>CH<sub>2</sub>PPh<sub>2</sub>)(OTf)<sub>2</sub> in CH<sub>2</sub>Cl<sub>2</sub>.<sup>87</sup> The structure of **46** was confirmed by <sup>1</sup>H and <sup>31</sup>P NMR spectroscopy and MALDI-TOF and ESI mass spectrometry. According to molecular modeling, the distance between the two adjacent Pt atoms in **46** is ~14 Å, and the distance between the two OCH<sub>2</sub>O bridges belonging to the upper and lower hemispheres is ~11.5 Å. The calculated internal volume is 1100 Å<sup>3</sup>.<sup>87</sup>

Another huge capsule **47**, with an internal volume of 950 Å<sup>3</sup> and sizeable portals, was constructed by Rebek and co-workers (Fig. 34).<sup>88</sup> The monomer is composed from four preformed glycoluril modules attached to a cavitand platform; self-assembled dimer **47** forms through sixteen hydrogen bonds. The large portals permit the solvent molecules to pass freely in and out of dimer **47**. However, more sizeable guests—cryptates of K<sup>+</sup>, Sr<sup>2+</sup>, and Ba<sup>2+</sup> salts—were entrapped, with the formation of kinetically stable complexes (NMR, ESI MS). This finding provides a rare example of so-called “complexes-within-complexes”.

The capsule's dimensions may also be enhanced by increasing the number of self-assembling components. As mentioned previously, co-crystallization of resorcinarene **2** and 4,4'-bipyridine from THF-EtOH-nitrobenzene mixture resulted in well-defined six-component capsular assembly **15** (Fig. 13).<sup>49</sup> It consists of six components held together by eight intermolecular O-H...N hydrogen bonds and eight intramolecular O-H...O hydrogen bonds; the cylindrical cavity of ~6 × 14.2 Å dimensions is reminiscent of a sealed hemicarcerand. Two



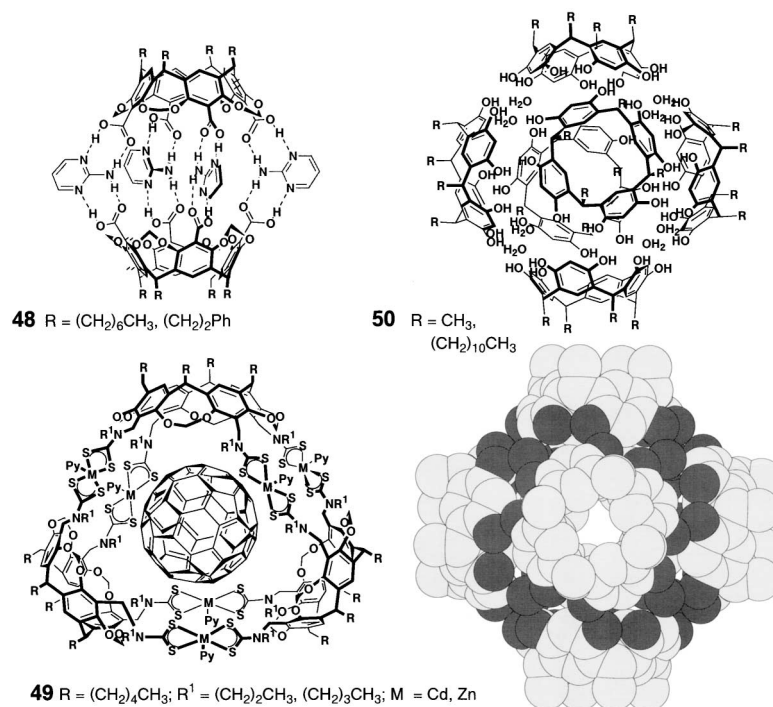
Fig. 34. Nanoscale self-assembling capsules **44–47**.<sup>80,84,87,88</sup>

molecules of nitrobenzene are encapsulated inside **15** in a head-to-head fashion, with aromatic rings directed into the resorcinarene cavities. Two cavitand tetracarboxylic acids and four 2-aminopyrimidines form a capsular structure **48** of  $9 \times 15$  Å dimensions (X-ray analysis).<sup>89</sup> Likewise, two nitrobenzene molecules were seen encapsulated inside in the solid state. From the NMR titration experiments in  $CDCl_3$ , it was concluded that capsule **48** is also stable in solution (Fig. 35).<sup>89</sup>

Spectacular trimeric assemblies **49** of cavitands functionalized with four dithiocarbamate units were obtained upon mixing with Zn(II) and Cd(II) salts in EtOH/H<sub>2</sub>O (Fig. 35).<sup>90</sup> In apolar solvents the <sup>1</sup>H NMR spectra are broad, but the complexes readily crystallized from pyridine/H<sub>2</sub>O and were characterized by X-ray crystallography. The trimers **49** form very stable 1:1 complexes with fullerene C<sub>60</sub> in benzene and toluene solutions; the log  $K_{ass}$  values are within the range 3.5–6 (UV-vis spectroscopy, 295 K). In the solid state, six molecules of resorcinarene **2** ( $R = Me$ ) and eight H<sub>2</sub>O molecules self-assemble into a spectacular spherical nanocavity **50** with a diameter of 17.7 Å and an internal volume of  $\sim 1375$  Å<sup>3</sup>.<sup>91</sup> Sixty hydrogen bonds hold the nanocavity together (Fig. 35). Although the presence of guest species was inferred from electron density maxima, they were not identified from the X-ray experiment. Molecular modeling, however, suggests that the

assembly is large enough to accommodate fullerenes or porphyrins. An even bigger self-assembled hexamer was observed in the solid state for tetrahydroxyresorcinarene.<sup>92</sup> According to the single crystal X-ray analysis, the shortest and the longest inner diameters for this hexamer were 14 and 19 Å, respectively, and the inner volume was  $\sim 1520$  Å<sup>3</sup>. This is one of the biggest self-assembled cavities prepared to date from organic materials. In total, seventy two HO...H–O intermolecular hydrogen bonds between the hydroxyresorcinarene hydroxyls hold the structure together, and, unlike with **50**, water molecules are not involved. Ten MeCN solvent molecules were entrapped inside upon crystallization.

One relatively unexplored direction in self-assembly of capsules is to employ hydrophobic solvents such as water to drive encapsulation of hydrophobic guests. For example, benzene, halobenzenes, chlorinated hydrocarbons, (cyclo)alkanes, and alcohols were successfully trapped by smaller, water-soluble Co(II) and Fe(II) resorcinarene-based cages in aqueous solution (pH > 5).<sup>93</sup> The main synthetic challenge here would be to build nanoscale water-soluble self-assembly modules, possessing hydrophobic interiors. Finally, the dissociation barrier for the encapsulation complexes may be increased through the introduction of additional binding sites within the cavity's interior.<sup>94</sup>

Fig. 35. Multi-component assemblies **48–50**<sup>89–91</sup> and the X-ray structure of **50**.<sup>91</sup>

## 9. Concluding Remarks

The notion of molecular containers emerged almost two decades ago. At that time, naturally occurring cyclodextrins were known as the only cavity-containing hosts able to accommodate smaller guests. The ambitious desire of chemists to have totally synthetic molecules permitting great structural variation and to control the cavity's size and shape led to the discovery of first man-made hollow containers in the early 1980s. Already then, inclusion complexes with small molecules were experimentally observed.<sup>95–97</sup> One of the earliest stable cryptophane complex, prepared by Collet, had the maximal internal dimension of  $\sim 8 \text{ \AA}$  and the cavity volume of  $95 \text{ \AA}^3$ , and entrapped just one  $CH_2Cl_2$  molecule.<sup>95</sup> Today, a wide variety of nanoscale molecular containers is available, and their inner spaces are unique. Their internal volumes are as high as  $1500 \text{ \AA}^3$ , and they may entrap guest molecules and ions which are up to  $20 \text{ \AA}$  long and more than  $700 \text{ Da}$  heavy. They may as well hold several, up to ten, guest species, which can even be different from each other. Both covalent bonds and noncovalent interactions have been effectively utilized to control size and shape of the interior nanocavities. The kinetic stability of the inclusion complexes may vary significantly but it can be controlled through the synthesis. The guest exchange can occur within milliseconds or can take hours or days. The uptake and release of guest species in some cases involves breaking the covalent bonds but sometimes just folding and unfolding of the host, which can be achieved by varying either solvent polarity or temperature, or both. It is now also possible to incorporate additional binding and catalytically active sites within the interior. The thermodynamics of the complexes may be improved as well. Combined with the rich and well-developed synthetic chemistry of calixarenes, this field un-

doubtedly has new horizons to be explored. The impact of nanoscale molecular containers in chemistry has been impressive and is expected to grow. Separation and sensing are the first visible priorities. Nanocavities have already been successfully used as receptors/sensors for industrially important substances such as substituted (hetero)aromatics and fullerenes. Biologically significant molecules and even some drugs have been complexed: examples with steroids, nucleotides, carbohydrates, adamantane derivatives have been mentioned. Nanocavities can encapsulate dyes for colorimetric sensing. For preparative organic chemistry, active reagents may be safely stored inside the capsule for a prolonged time and released upon facile control. Various problems of physical organic chemistry are being approached as well. Nanocavity's use as NMR shift reagents is promising. In some cases, significant upfield NMR shifts of the entrapped molecules offers the possibility to deduce their structural features "from inside", to determine the orientation of the guests and their interaction with each other and the receptor's interior walls. In principle, such host-guest complexes can be used for the structural information/memory storage; some communication between two entrapped guests has been detected as well. Stabilization of reactive intermediates is another important area under investigation. Moreover, as two or even more guests are encapsulated, reaction/catalytic chambers are on the way. In biochemistry and molecular biology, nanoscale containers are aiming at drug encapsulation, drug active transport through the cell membranes and drug delivery. Approaches towards water-soluble, polymeric nanocavities and even novel, cavity-based materials have been introduced.<sup>98</sup> Construction and application of novel architectures offer even wider perspectives.

I am grateful to The University of Texas at Arlington for fi-

nancial support. The Skaggs Research Foundation at The Scripps Research Institute is kindly acknowledged for supporting initial stages of this work. This account is dedicated to Prof. David N. Reinhoudt on the occasion of his upcoming 60th birthday.

## References

- 1 a) D. J. Cram and J. M. Cram, *Science*, **183**, 803 (1974). b) D. J. Cram, *Science*, **219**, 1177 (1983). c) D. J. Cram, *Angew. Chem., Int. Ed. Engl.*, **27**, 1009 (1988). d) D. J. Cram, *Nature*, **356**, 29 (1992).
- 2 F. D. Cramer, *Rev. Pure Appl. Chem.*, **5**, 143 (1955).
- 3 D. J. Cram and J. M. Cram, "Container Molecules and their Guests," Royal Society of Chemistry, Cambridge (1994).
- 4 Review collection: *Chem. Rev.*, **98**, 1741-2076 (1998).
- 5 F. Diederich, "Cyclophanes," Royal Society of Chemistry, Cambridge (1991).
- 6 C. Seel and F. Vögtle, *Angew. Chem., Int. Ed. Engl.*, **31**, 528 (1992).
- 7 J. Rebek, Jr., *Angew. Chem., Int. Ed. Engl.*, **29**, 245 (1990).
- 8 a) J. R. Moran, S. Karbach, and D. J. Cram, *J. Am. Chem. Soc.*, **104**, 5826 (1982). b) R. C. Helgeson, M. Lauer, and D. J. Cram, *J. Chem. Soc., Chem. Commun.*, **1983**, 101.
- 9 D. J. Cram, S. Karbach, Y. H. Kim, L. Baczynskyj, and G. W. Kallemeyn, *J. Am. Chem. Soc.*, **107**, 2575 (1985).
- 10 a) M. E. Tanner, C. B. Knobler, and D. J. Cram, *J. Am. Chem. Soc.*, **112**, 1659 (1990). b) D. J. Cram, M. E. Tanner, and C. B. Knobler, *J. Am. Chem. Soc.*, **113**, 7717 (1991). See also Ref. 22.
- 11 M. M. Conn and J. Rebek, Jr., *Chem. Rev.*, **97**, 1647 (1997).
- 12 Recent review on self-assembly: D. Philp and J. F. Stoddart, *Angew. Chem., Int. Ed. Engl.*, **35**, 1154 (1996).
- 13 Cavitands: D. M. Rudkevich and J. Rebek, Jr., *Eur. J. Org. Chem.*, **1999**, 1991.
- 14 Carcerands and hemicarcerands: a) A. Jasat and J. C. Sherman, *Chem. Rev.*, **99**, 931 (1999). b) R. Warmuth and J. Yoon, *Acc. Chem. Res.*, **34**, 95 (2001). Structural classification: c) L. R. MacGillivray and J. L. Atwood, *Angew. Chem., Int. Ed.*, **38**, 1019 (1999). Cryptophanes: d) A. Collet, J.-P. Dutasta, B. Lozach, and J. Canceill, *Top. Curr. Chem.*, **165**, 103 (1993).
- 15 Self-assembling capsules: a) J. de Mendoza, *Chem.-Eur. J.*, **4**, 1373 (1998). b) J. Rebek, Jr., *Acc. Chem. Res.*, **32**, 278-286 (1999).
- 16 Reactions inside cavities: a) K. Goto and R. Okazaki, *Liebigs Ann./Recl.*, **1997**, 2393. b) R. Warmuth, *Eur. J. Org. Chem.*, **2001**, 423.
- 17 Imprinted polymers: B. Sellergren, *Angew. Chem., Int. Ed.*, **39**, 1031 (2000). Dendrophanes: D. K. Smith and F. Diederich, *Top. Curr. Chem.*, **210**, 183 (2000).
- 18 D. D. Lasic and D. Papahadjopoulos, *Science*, **267**, 1275 (1995), and literature therein.
- 19 A. Corma and H. Garcia, *J. Chem. Soc., Dalton Trans.*, **2000**, 1381.
- 20 a) P. G. Schultz and R. A. Lerner, *Science*, **269**, 1835 (1995). b) P. G. Schultz, *Proc. Natl. Acad. Sci. U.S.A.*, **95**, 14590 (1998), and references therein.
- 21 J.-M. Lehn, "Supramolecular Chemistry: Concepts and Perspectives," VCH, Weinheim-New York-Basel-Cambridge-Tokyo (1995).
- 22 D. J. Cram, M. T. Blanda, K. Paek, and C. B. Knobler, *J. Am. Chem. Soc.*, **114**, 7765 (1992).
- 23 In the analysis of structural data and in the preparation of figures, we used MacroModel 7.0; Amber\* Force Field.
- 24 Recent reviews: a) C. D. Gutsche, "Calixarenes Revisited," Royal Society of Chemistry, Cambridge (1998). b) V. Böhmer, *Angew. Chem., Int. Ed. Engl.*, **34**, 713 (1995). Resorcinarenes: c) P. Timmerman, W. Verboom, and D. N. Reinhoudt, *Tetrahedron*, **52**, 2663 (1996). d) A. Ikeda and S. Shinkai, *Chem. Rev.*, **97**, 1713 (1997). Homocalixarenes: e) S. Ibach, V. Prautzsch, F. Vögtle, C. Chartroux, and K. Gloe, *Acc. Chem. Res.*, **32**, 729 (1999).
- 25 C. D. Gutsche, *Acc. Chem. Res.*, **16**, 161 (1983). Here, it is proposed to use calixarene cavities as enzyme mimics.
- 26 a) D. J. Cram, S. Karbach, H.-E. Kim, C. B. Knobler, E. F. Maverick, J. L. Ericson, and R. C. Helgeson, *J. Am. Chem. Soc.*, **110**, 2229 (1988). b) D. J. Cram, K. D. Stewart, I. Goldberg, and K. N. Trueblood, *J. Am. Chem. Soc.*, **107**, 2574 (1985). c) J. A. Tucker, C. B. Knobler, K. N. Trueblood, and D. J. Cram, *J. Am. Chem. Soc.*, **111**, 3688 (1989).
- 27 A. Arduini, W. M. McGregor, D. Paganuzzi, A. Pochini, A. Secchi, F. Ugozzoli, and R. Ungaro, *J. Chem. Soc., Perkin Trans. 2*, **1996**, 839. Calix[4]arene tetraesters and tetraamides also exist as C<sub>4v</sub> conformers when they complex sodium and potassium.
- 28 C. D. Gutsche and P. F. Pagoria, *J. Org. Chem.*, **50**, 5795 (1985).
- 29 a) R. K. Juneja, K. D. Robinson, C. P. Johnson, and J. L. Atwood, *J. Am. Chem. Soc.*, **115**, 3818 (1993) and references therein. b) C. A. Gleave and I. O. Sutherland, *J. Chem. Soc., Chem. Commun.*, **1994**, 1873. c) B. Xu, Y.-J. Miao, and T. M. Swager, *J. Org. Chem.*, **63**, 8561 (1998), and references therein. See also Refs. 28 and 97.
- 30 C. von dem Bussche-Hünnefeld, R. C. Helgeson, D. Bühring, C. B. Knobler, and D. J. Cram, *Croat. Chem. Acta*, **69**, 1447 (1996).
- 31 a) S. Ma, D. M. Rudkevich, and J. Rebek, Jr., *J. Am. Chem. Soc.*, **120**, 4977 (1998). b) D. M. Rudkevich and J. Rebek, Jr., in: "Calixarenes for Separation," ed by G. J. Lumetta, R. D. Rogers, and A. S. Gopalan, ACS Symposium Series, **757**, 270 (2000).
- 32 L. Sebo, F. Diederich, and V. Gramlich, *Helv. Chim. Acta*, **83**, 93 (2000).
- 33 a) H. Xi, C. L. D. Gibb, E. D. Stevens, and B. C. Gibb, *Chem. Commun.*, **1998**, 1743. b) H. Xi, C. L. D. Gibb, and B. C. Gibb, *J. Org. Chem.*, **64**, 9286 (1999). c) J. O. Green, J.-H. Baird, and B. C. Gibb, *Org. Lett.*, **2**, 3845 (2000).
- 34 a) P. Soncini, S. Bonsignore, E. Dalcaneale, and F. Ugozzoli, *J. Org. Chem.*, **57**, 4608 (1992). b) M. Vincenti, C. Minero, E. Pelizzetti, A. Secchi, and E. Dalcaneale, *Pure Appl. Chem.*, **67**, 1075 (1995).
- 35 J. R. Moran, J. L. Ericson, E. Dalcaneale, J. A. Bryant, C. B. Knobler, and D. J. Cram, *J. Am. Chem. Soc.*, **113**, 5707 (1991).
- 36 F. C. Tucci, D. M. Rudkevich, and J. Rebek, Jr., *J. Org. Chem.*, **64**, 4555 (1999).
- 37 K. T. Chapman and W. C. Still, *J. Am. Chem. Soc.*, **111**, 3075 (1989).
- 38 D. J. Cram, H.-J. Choi, J. A. Bryant, and C. B. Knobler, *J. Am. Chem. Soc.*, **114**, 7748 (1992).
- 39 a) D. M. Rudkevich, G. Hilmersson, and J. Rebek, Jr., *J. Am. Chem. Soc.*, **120**, 12216 (1998). b) A. Shivanyuk, K. Rissanen, S. K. Körner, D. M. Rudkevich, and J. Rebek, Jr., *Helv. Chim. Acta*, **83**, 1778 (2000).
- 40 O. Mogck, M. Pons, V. Böhmer, and W. Vogt, *J. Am. Chem. Soc.*, **119**, 5706 (1997).
- 41 D. J. Cram, M. E. Tanner, and C. B. Knobler, *J. Am. Chem.*

- Soc.*, **113**, 7717 (1991). See also Refs. 14 and 59. For slow de-complexation at 295 K see Ref. 63.
- 42 U. Lücking, F. C. Tucci, D. M. Rudkevich, and J. Rebek, Jr., *J. Am. Chem. Soc.*, **122**, 8880 (2000).
- 43 A. R. Renslo, F. C. Tucci, D. M. Rudkevich, and J. Rebek, Jr., *J. Am. Chem. Soc.*, **122**, 4573 (2000).
- 44 A. R. Renslo and J. Rebek, Jr., *Angew. Chem., Int. Ed.*, **39**, 3281 (2000).
- 45 U. Lücking, D. M. Rudkevich, and J. Rebek, Jr., *Tetrahedron Lett.*, **41**, 9547 (2000).
- 46 S. D. Starnes, D. M. Rudkevich, and J. Rebek, Jr., *Org. Lett.*, **2**, 1995 (2000).
- 47 C. L. D. Gibb, E. D. Stevens, and B. C. Gibb, *J. Am. Chem. Soc.*, **123**, 5849 (2001).
- 48 a) L. R. MacGillivray and J. L. Atwood, *J. Am. Chem. Soc.*, **119**, 6931 (1997). b) L. R. MacGillivray and J. L. Atwood, *Chem. Commun.*, **1999**, 181. c) L. R. MacGillivray, H. A. Spinney, J. L. Reid, and J. A. Ripmeester, *Chem. Commun.*, **2000**, 517. d) L. R. MacGillivray, J. L. Reid, and J. A. Ripmeester, *CrystEngComm*, **1**, (1999).
- 49 L. R. MacGillivray, P. R. Diamante, J. L. Reid, and J. A. Ripmeester, *Chem. Commun.*, **2000**, 359. Even larger capsule was very recently obtained from resorcinarene **2** and terpyridine; four toluene or two toluene and two diethyl ether molecules were found encapsulated. See: G. W. V. Cave, M. J. Hardie, B. A. Roberts, and C. L. Raston, *Eur. J. Org. Chem.*, **2001**, 3227.
- 50 A. Arduini, A. Pochini, and A. Secchi, *Eur. J. Org. Chem.*, **2000**, 2325. Conformationally flexible analogs: K. Araki, K. Hiseichi, T. Kanai, and S. Shinkai, *Chem. Lett.*, **1995**, 569.
- 51 J. Wang, S. G. Bodige, W. H. Watson, and C. D. Gutsche, *J. Org. Chem.*, **65**, 8260 (2000).
- 52 J. Wang and C. D. Gutsche, *J. Am. Chem. Soc.*, **120**, 12226 (1998).
- 53 T. Haino, M. Yanase, and Y. Fukazawa, *Angew. Chem., Int. Ed.*, **37**, 997 (1998).
- 54 R. G. Chapman and J. C. Sherman, *J. Am. Chem. Soc.*, **120**, 9818 (1998).
- 55 a) D. J. Cram, L. M. Tunstad, and C. B. Knobler, *J. Org. Chem.*, **57**, 528 (1992). b) L. M. Tunstad, J. E. Nunez, S.-W. Kang, and C. E. Godinez, 219th ACS National Meeting, San Francisco, CA, March 26-30, 2000, Abstr., p. 111.
- 56 a) I. Higler, P. Timmerman, W. Verboom, and D. N. Reinhoudt, *J. Org. Chem.*, **61**, 5920 (1996). b) I. Higler, W. Verboom, F. C. J. M. van Veggel, F. de Jong, and D. N. Reinhoudt, *Liebigs Ann./Recueil*, **1997**, 1577.
- 57 S. D. Starnes, D. M. Rudkevich, and J. Rebek, Jr., *J. Am. Chem. Soc.*, **123**, 4659 (2001).
- 58 J. A. Bryant, M. T. Blanda, M. Vincenti, and D. J. Cram, *J. Am. Chem. Soc.*, **113**, 2167 (1991).
- 59 T. A. Robbins, C. B. Knobler, D. R. Bellew, and D. J. Cram, *J. Am. Chem. Soc.*, **116**, 111 (1994).
- 60 H.-J. Choi, D. Bühring, M. L. C. Quan, C. B. Knobler, and D. J. Cram, *J. Chem. Soc., Chem. Commun.*, **1992**, 1733.
- 61 N. Chopra and J. C. Sherman, *Angew. Chem., Int. Ed.*, **38**, 1955 (1999).
- 62 M. L. C. Quan and D. J. Cram, *J. Am. Chem. Soc.*, **113**, 2754 (1991).
- 63 D. J. Cram, R. Jaeger, and K. Deshayes, *J. Am. Chem. Soc.*, **115**, 10111 (1993).
- 64 C. von dem Bussche-Hünnefeld, D. Bühring, C. B. Knobler, and D. J. Cram, *J. Chem. Soc., Chem. Commun.*, **1995**, 1085.
- 65 C. L. D. Gibb, E. D. Stevens, and B. C. Gibb, *Chem. Commun.*, **2000**, 363.
- 66 P. Timmerman, K. G. A. Nierop, E. A. Brinks, W. Verboom, F. C. J. M. van Veggel, W. P. van Hoorn, and D. N. Reinhoudt, *Chem. Eur. J.*, **1**, 132 (1995).
- 67 S. Mecozzi and J. Rebek, Jr., *Chem. Eur. J.*, **4**, 1016 (1998).
- 68 Cavitands: T. Haino, D. M. Rudkevich, A. Shivanyuk, K. Rissanen, and J. Rebek, Jr., *Chem. Eur. J.*, **6**, 3797 (2000). Hemispherands: E. L. Piatnitski, R. A. Flowers II, and K. Deshayes, *Chem. Eur. J.*, **6**, 999 (2000).
- 69 D. M. Rudkevich, W. T. S. Huck, F. C. J. M. van Veggel, and D. N. Reinhoudt, in "Transition Metals in Supramolecular Chemistry," ed by L. Fabbrizzi and A. Poggi, Kluwer Academic Publishers, Dordrecht, Boston, London (1994), pp. 329-349.
- 70 S. Anderson, H. L. Anderson, A. Bashall, M. McPartlin, and J. K. M. Sanders, *Angew. Chem., Int. Ed. Engl.*, **34**, 1096 (1995).
- 71 S.-K. Chang, D. Van Engen, E. Fan, and A. D. Hamilton, *J. Am. Chem. Soc.*, **113**, 7640 (1991).
- 72 S. Ro, S. J. Rowan, A. R. Pease, D. J. Cram, and J. F. Stoddart, *Org. Lett.*, **2**, 2411 (2000). Dynamic covalent chemistry: J.-M. Lehn, *Chem. Eur. J.*, **5**, 2455 (1999).
- 73 N. Chopra and J. C. Sherman, *Angew. Chem., Int. Ed. Engl.*, **36**, 1727 (1997).
- 74 N. Chopra, C. Naumann, and J. C. Sherman, *Angew. Chem., Int. Ed.*, **39**, 194 (2000).
- 75 Z. Zhong, A. Ikeda, and S. Shinkai, *J. Am. Chem. Soc.*, **121**, 11906 (1999).
- 76 D. M. Rudkevich, in "Calixarenes 2001," ed by Z. Asfari, V. Böhmer, J. M. Harrowfield, and J. Vicens, Kluwer Academic Publishers, Dordrecht (2001), pp. 155-180.
- 77 a) K. D. Shimizu and J. Rebek, Jr., *Proc. Natl. Acad. Sci. U.S.A.*, **92**, 12403 (1995). b) O. Mogck, V. Böhmer, and W. Vogt, *Tetrahedron*, **52**, 8489 (1996).
- 78 One spectacular exception is "soft-ball" which has an internal volume of 320 Å<sup>3</sup> and can accommodate two benzene molecules, see: R. Meissner, X. Garcias, S. Mecozzi, and J. Rebek, Jr., *J. Am. Chem. Soc.*, **119**, 77 (1997).
- 79 Y. L. Cho, D. M. Rudkevich, and J. Rebek, Jr., *J. Am. Chem. Soc.*, **122**, 9868 (2000).
- 80 S. K. Körner, F. C. Tucci, D. M. Rudkevich, T. Heinz, and J. Rebek, Jr., *Chem. Eur. J.*, **6**, 187 (2000).
- 81 T. Heinz, D. M. Rudkevich, and J. Rebek, Jr., *Nature*, **394**, 764 (1998).
- 82 T. Heinz, D. M. Rudkevich, and J. Rebek, Jr., *Angew. Chem., Int. Ed.*, **38**, 1136 (1999).
- 83 F. C. Tucci, D. M. Rudkevich, and J. Rebek, Jr., *J. Am. Chem. Soc.*, **121**, 4928 (1999).
- 84 A. Ikeda, M. Yoshimura, H. Udzu, C. Fukuhara, and S. Shinkai, *J. Am. Chem. Soc.*, **121**, 4296 (1999).
- 85 A. Ikeda, H. Udzu, M. Yoshimura, and S. Shinkai, *Tetrahedron*, **56**, 1825 (2000).
- 86 Z. Zhong, A. Ikeda, M. Ayabe, S. Shinkai, S. Sakamoto, and K. Yamaguchi, *J. Org. Chem.*, **66**, 1002 (2001).
- 87 N. Cuminetti, M. H. K. Ebbing, P. Prados, J. de Mendoza, and E. Dalcanele, *Tetrahedron Lett.*, **42**, 527 (2001).
- 88 A. Lützen, A. R. Renslo, C. A. Schalley, B. M. O'Leary, and J. Rebek, Jr., *J. Am. Chem. Soc.*, **121**, 7455 (1999).
- 89 K. Kobayashi, T. Shirasaka, K. Yamaguchi, S. Sakamoto, E. Horn, and N. Furukawa, *Chem. Commun.*, **2000**, 41.
- 90 O. D. Fox, M. G. B. Drew, E. J. S. Wilkinson, and P. D. Beer, *Chem. Commun.*, **2000**, 391.

- 91 L. R. MacGillivray and J. L. Atwood, *Nature*, **389**, 469 (1997). For the very recent solution studies, see: A. Shivanyuk and J. Rebek, Jr., *Proc. Natl. Acad. Sci. U.S.A.*, **98**, 7662 (2001)
- 92 T. Gerkenmeier, W. Iwanek, C. Agena, R. Fröhlich, S. Kotila, C. Näther, and J. Mattay, *Eur. J. Org. Chem.*, **1999**, 2257.
- 93 a) O. D. Fox, J. F.-Y. Leung, J. M. Hunter, N. K. Dalley, and R. G. Harrison, *Inorg. Chem.*, **39**, 783 (2000). b) O. D. Fox, N. K. Dalley, and R. G. Harrison, *Inorg. Chem.*, **38**, 5860 (1999).
- 94 Self-assembling metalloporphyrins and phthalocyanines: a) Y. Kuroda, A. Kawashima, Y. Hayashi, and H. Ogoshi, *J. Am. Chem. Soc.*, **119**, 4929 (1997). b) A. Lützen, S. D. Starnes, D. M. Rudkevich, and J. Rebek, Jr., *Tetrahedron Lett.*, **41**, 3777 (2000).
- 95 First cryptophanes: a) J. Gabard and A. Collet, *J. Chem. Soc., Chem. Commun.*, **1981**, 1137. b) J. Canceill, M. Cesario, A. Collet, J. Guilhem, and C. Pascard, *J. Chem. Soc., Chem. Commun.*, **1985**, 361 (X-ray studies). c) J. Canceill, L. Lacombe, and A. Collet, *J. Am. Chem. Soc.*, **107**, 6993 (1985) (solution studies).
- 96 First speleands: J. Canceill, A. Collet, J. Gabard, F. Kotzyba-Hibert, and J.-M. Lehn, *Helv. Chim. Acta*, **65**, 1894 (1982).
- 97 For an early study of calixarene complexes in solution, see: L. J. Bauer and C. D. Gutsche, *J. Am. Chem. Soc.*, **107**, 6063 (1985).
- 98 Self-assembling monolayers of cavitopes, hemicarceplexes, and large hydrophobic surfaces on gold: a) E. U. Thoden van Velzen, J. F. J. Engbersen, and D. N. Reinhoudt, *J. Am. Chem. Soc.*, **116**, 3597 (1994). b) B.-H. Huisman, D. M. Rudkevich, A. Farrán, W. Verboom, F. C. J. M. van Veggel, and D. N. Reinhoudt, *Eur. J. Org. Chem.*, **2000**, 269. c) A. Friggeri, F. C. J. M. van Veggel, and D. N. Reinhoudt, *Chem. Eur. J.*, **5**, 3595 (1999). Polymer-supported cavitands: A. Rafai Far, D. M. Rudkevich, T. Haino, and J. Rebek, Jr., *Org. Lett.*, **2**, 3465 (2000).



Dmitry M. Rudkevich was born in the country of Ukraine in 1963. He studied chemistry at the Institute of Organic Chemistry, National Academy of Sciences of the Ukraine, with the late Prof. Leonid N. Markovsky. In 1992–1995 he worked in the laboratory of Prof. David N. Reinhoudt at the University of Twente in the Netherlands. He holds a Ph. D. in chemistry from the University of Twente. In 1996 Dr. Rudkevich moved to the United States to work with Prof. Julius Rebek, Jr., first at the Massachusetts Institute of Technology and later at The Scripps Research Institute in La Jolla, California. In 1997–2001, he was a Research Assistant Professor of the Skaggs Institute for Chemical Biology at Scripps. Currently, Dr. Rudkevich is on the faculty at the Department of Chemistry and Biochemistry, The University of Texas at Arlington. His research interests deal with molecular recognition. Dr. Rudkevich is a co-author of 90 scientific papers on the design and synthesis of macrocycles, clefts, cavitands, capsules, and superstructured porphyrins; complexation studies with ions and neutral molecules; hydrogen bonding and self-assembly.